

STEERING DIFFUSION MODELS TOWARDS CREDIBLE CONTENT RECOMMENDATION

000
001
002
003
004
005
006
007
008
009
010
011
012
013
014
015
016
017
018
019
020
021
022
023
024
025
026
027
028
029
030
031
032
033
034
035
036
037
038
039
040
041
042
043
044
045
046
047
048
049
050
051
052
053
Anonymous authors
Paper under double-blind review

ABSTRACT

In recent years, diffusion models (DMs) have achieved remarkable success in recommender systems (RSs), owing to their strong capacity to model the complex distributions of item content and user behaviors. Despite their effectiveness, existing methods pose the danger of generating uncredible content recommendations (e.g., fake news, misinformation) that may significantly harm social well-being, as they primarily emphasize recommendation accuracy while neglecting the credibility of the recommended content. To address this issue, in this paper, we propose **Disco**, a novel method to steer diffusion models towards credible content recommendation. Specifically, we design a novel disentangled diffusion model to mitigate the harmful influence of uncredible content on the generation process while preserving high recommendation accuracy. This is achieved by reformulating the diffusion objective to encourage generation conditioned on preference-related signals while discouraging generation conditioned on uncredible content-related signals. In addition, to further improve the recommendation credibility, we design a progressively enhanced credible subspace projection that suppresses uncredible content by projecting diffusion targets into the null space of uncredible content. Extensive experiments on real-world datasets demonstrate the effectiveness of **Disco** in terms of both accurate and credible content recommendations.

1 INTRODUCTION

Diffusion models (DMs) have achieved remarkable advances across multiple domains, such as image synthesis (Ho et al., 2020; Dhariwal & Nichol, 2021) and language/text generation (Li et al., 2022; Lovelace et al., 2023). Owing to their strong capability in modeling complex data distributions of user behaviors and diverse item content types (e.g., text, images, and videos), DMs have attracted growing attention in recommender systems (RSs), thereby further driving the innovations in this field (Wang et al., 2023b; Yang et al., 2023b; Liu et al., 2025a).

DM-based recommendation methods generally adopt a diffusion-then-denoising paradigm to model the distributions of users' behaviors and then generate items they are likely to engage with (Yang et al., 2023b; Liu et al., 2025a; Li et al., 2023). Figure 1 illustrates the overall process of existing DM-based methods. A sequence encoder (e.g., Transformer (Vaswani et al., 2017), GRU (Chung et al., 2014)) is first employed to encode the embeddings of the first $(n - 1)$ context items interacted by a user into a unified representation of the user's overall preference, which serve as the condition in the reverse stage. The n -th item (i.e., the last item interacted with by the user) is then treated as the diffusion target. In the forward process, noise is gradually added to the diffusion target according to a predefined noise schedule. In the reverse process, the sequence encoder's output serves as the condition to guide the generation of the item embeddings that reflect users' genuine preferences (Li et al., 2025b; Cai et al., 2025).

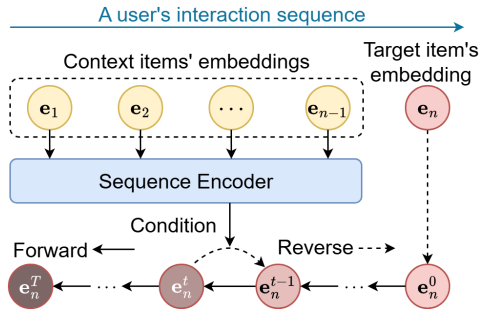


Figure 1: A general paradigm of DM-based sequential recommendation methods. The condition and diffusion target (i.e., target item's embedding) are two core components in DM-based methods.

054 Although DM-based recommendation methods have achieved remarkable success, they often over-
 055 look a critical real-world concern: **the risk of generating uncredible content recommendations**
 056 **that can harm social well-being**. For example, news RSs powered by DMs may produce uncred-
 057 ible recommendations containing fake news (Wang et al., 2022; 2024a), as these methods typically
 058 overlook the credibility of recommended content. Recommending such uncredible content to users
 059 not only diminishes users' experience but also poses substantial societal risks. For instance, during
 060 the COVID-19 pandemic, news RSs (e.g., online news portals) were shown to amplify the spread
 061 of health-related fake news (e.g., false cures and vaccine conspiracy theories), which fueled public
 062 confusion and resistance to medical treatments (Loomba et al., 2021). Hence, from a societal con-
 063 sideration perspective, it is crucial to develop DM tailored for credible content recommendations.

064 To achieve this goal, we first conduct both empirical and theoretical analysis to investigate why
 065 existing DM-based recommendation methods risk generating uncredible content recommendations.
 066 The detailed analysis can be found in Appendix C. Our analysis reveals two key factors: **(1) un-**
 067 **credible condition**, which arises when a user has previously interacted with uncredible items (i.e.,
 068 there are uncredible items in context items); and **(2) uncredible diffusion target**, which occurs when
 069 the target item itself is uncredible. In this paper, an uncredible item refers to an item containing
 070 uncredible content, such as fake news and misinformation. These two factors jointly lead existing
 071 DM-based methods to generate recommendations that may contain uncredible content.

072 Hence, to develop a diffusion model tailed for credible content recommendation, it is necessary to
 073 carefully address these two factors. A straightforward solution is to remove uncredible items from
 074 both context items and diffusion targets, or to apply recommendation unlearning methods (Chen
 075 et al., 2022; Zhang et al., 2024) to erase their impacts. This can ensure the credibility of both the
 076 condition and the diffusion target. However, such an approach raises a critical issue: uncredible
 077 items may still reflect users' genuine preferences. For instance, if a user reads a sports-related
 078 fake news article, it may signal this user's underlying interest in sports topics. In this case, remov-
 079 ing the uncredible items entirely would severely harm recommendation accuracy. Thus, **the first**
 080 **challenge lies in how to mitigate the negative impact of uncredible content without sacrificing**
 081 **recommendation accuracy**. An alternative solution is to retain users' preference-related informa-
 082 tion while removing only the uncredible aspects of content items. However, this approach requires
 083 rich supervision (i.e., credibility labels) to ensure accurate and comprehensive removal. In practice,
 084 only a small portion of items are verified and labeled. For example, on news portals, some articles
 085 may be flagged as fake, while many others remain unverified. Hence, **the second challenge is how**
 086 **to develop a diffusion model that can effectively handle both known and unknown uncredible**
 087 **content under limited label availability**. Existing methods for credible content recommendation
 088 (Wang et al., 2022; 2024a; Ma et al., 2025) typically assume that all uncredible items are fully
 089 labeled, which rarely holds in real-world scenarios, leading to suboptimal performance.

090 To overcome these two challenges and steer diffusion models towards credible content
 091 recommendation, we propose a novel framework called *Disco*. Specifically, **to address the un-**
 092 **credible condition and the challenge of preserving recommendation accuracy**, we design a dis-
 093 entangled diffusion model that separates uncredible content from users' preference-related infor-
 094 mation in items' embeddings. With this disentanglement, the generation process becomes free from
 095 the harmful influence of uncredible items, while still preserving high recommendation accuracy by
 096 retaining users' genuine preference-related information. In addition, instead of incorporating auxil-
 097 iary disentanglement networks and constraints which often introduce extra computation cost (Wang
 098 et al., 2023c; Qi et al., 2024; Wang et al., 2022; Ma et al., 2025), the diffusion model itself can
 099 serve as an effective disentangler with proper adjustments. Specifically, we reformulate the diffu-
 100 sion objective to encourage the model generation guided by preference-related signals (i.e., **signals**
 101 **indicating users' preference, such as content topics**), while discouraging the generation conditioned
 102 on uncredible content-related signals (i.e., **uncredible signals such as inaccurate and misleading**
 103 **information**). **To address the uncredible diffusion target**, we introduce a credible subspace pro-
 104 **jection module** to project diffusion targets into the null space of uncredible content features, which
 105 maximally excludes uncredible information. **To overcome the challenge of limited labeled data**,
 106 the uncredible content features are progressively enhanced by detecting and incorporating potential
 107 uncredible items, making the null space projection progressively more accurate and comprehensive.
 108 Comprehensive experiments verify the effectiveness of *Disco* in terms of delivering both accurate
 109 and credible content recommendations.

110 In summary, our contributions can be concluded as follows:

- 108 • We propose **Disco**, a novel diffusion model tailored for credible content recommendation. **To**
109 **the best of our knowledge, Disco is the first work designed for credible content recommendation**
110 **under conditions of limited credibility labels.**
- 111 • A novel disentangled diffusion model is designed to mitigate the recommendations of uncredible
112 content while preserving high recommendation accuracy.
- 113 • We propose a new progressively enhanced credible subspace projection to further suppress and
114 mitigate the harmful impacts of uncredible content contained in diffusion targets.
- 115 • Comprehensive experiments on three real-world datasets demonstrate the effectiveness of **Disco**
116 in generating both accurate and credible content recommendation.

118 2 PRELIMINARY

120 2.1 CREDIBLE CONTENT RECOMMENDATION

122 **Content recommendation.** The content recommendation task in this paper follows the sequential
123 recommendation paradigm (Wang et al., 2019; Zhang et al., 2018), which aims to infer users' potential
124 interests based on their chronologically ordered interaction sequences with content items (e.g.,
125 news, and videos and movies) (Wu et al., 2023a; Deldjoo et al., 2016; Goyani & Chaurasiya, 2020).
126 The set of all sequences is denoted as $\mathcal{S} = \{s_1, s_2, \dots, s_{|\mathcal{S}|}\}$, where each sequence is represented
127 as $s = \{i_1, \dots, i_{n-1}, i_n\}$ ($s \in \mathcal{S}$). Here, $\{i_1, \dots, i_{n-1}\}$ are the context items, and i_n is the target item.
128 Each content item i_k is transformed into an embedding vector \mathbf{e}_k using modality-specific
129 feature extractors, such as language models for textual content or visual encoders for images and
130 videos, yielding a sequence of embeddings $\{\mathbf{e}_1, \dots, \mathbf{e}_n\}$. Given a user's historical sequence s , the
131 goal is to generate a personalized ranking over a set of candidate content items and predict the next
132 item that the user is most likely to engage with (Kang & McAuley, 2018).

133 **Credible content recommendation.** In this paper, we formulate the task of credible content recommendation as mitigating the exposure of users to uncredible items (Wang et al., 2022; 2024a).
134 A recommendation model is considered more credible if its generated recommendation lists contain
135 smaller proportions of uncredible items. uncredible items include uncredible information like
136 fake news and misinformation, which often degrades user experience and leads to adverse societal
137 impacts. Moreover, we focus on a more challenging setting in which only partial credibility labels
138 indicating whether an item contains uncredible content are available during training, reflecting
139 the practical difficulty of obtaining exhaustive annotations in real-world RSs. In contrast, complete
140 labels are provided during testing to ensure an accurate evaluation.

143 **Definition 1 Content credibility.** Content credibility indicates whether an item contains uncredible
144 information such as false, misleading, or inaccurate content. Items containing such information are
145 regarded uncredible (e.g., fake news, misinformation), whereas all others are regarded credible.

147 2.2 DIFFUSION MODELS FOR SEQUENTIAL RECOMMENDATION

149 In sequential recommendation scenarios, DMs are generally utilized on the embedding of the last
150 item (i.e., \mathbf{e}_n) in a sequence (Yang et al., 2023b; Liu et al., 2025a). The detailed process is as follows:

152 **In the forward stage**, DMs gradually add Gaussian noise to embedding \mathbf{e}_n according to a noise
153 schedule $[\beta_1, \dots, \beta_T]$:

$$154 q(\mathbf{e}_n^t | \mathbf{e}_n^{t-1}) = \mathcal{N}(\mathbf{e}_n^t; \sqrt{1 - \beta_t} \mathbf{e}_n^{t-1}, \beta_t \mathbf{I}), \quad q(\mathbf{e}_n^t | \mathbf{e}_n^0) = \mathcal{N}(\mathbf{e}_n^t; \sqrt{\bar{\alpha}_t} \mathbf{e}_n^0, (1 - \bar{\alpha}_t) \mathbf{I}), \quad (1)$$

155 where $\mathbf{e}_n^0 = \mathbf{e}_n$, $\alpha_t = 1 - \beta_t$ and $\bar{\alpha}_t = \prod_{s=1}^T \alpha_s$. The first equation is the step-by-step Markov
156 process from \mathbf{e}_n^{t-1} to \mathbf{e}_n^t . The second equation is derived based on the Markov chain principle (Ho
157 et al., 2020), which can be used to directly derive \mathbf{e}_n^t from \mathbf{e}_n^0 in one step. A reparameterization trick
158 is then applied to obtain variable $\mathbf{e}_n^t = \sqrt{\bar{\alpha}_t} \mathbf{e}_n^0 + \sqrt{1 - \bar{\alpha}_t} \epsilon$, where $\epsilon \sim \mathcal{N}(\mathbf{0}, \mathbf{I})$.

159 **In the reverse stage**, DMs progressively recover the diffusion target step by step starting from a
160 Gaussian noise $p(\mathbf{e}_n^T) = \mathcal{N}(\mathbf{0}, \mathbf{I})$:

$$161 p_\theta(\mathbf{e}_n^{t-1} | \mathbf{e}_n^t, \mathbf{c}) = \mathcal{N}(\mathbf{e}_n^{t-1}; \boldsymbol{\mu}_\theta(\mathbf{e}_n^t, \mathbf{c}, t), \boldsymbol{\Sigma}_\theta(\mathbf{e}_n^t, \mathbf{c}, t)), \quad (2)$$

162 where $\Sigma_\theta(\mathbf{e}_n^t, \mathbf{c}, t)$ is fixed to $\sigma^2(t) = \frac{1-\bar{\alpha}_{t-1}}{1-\bar{\alpha}_t} \beta_t$ following the common practice in previous work
 163 (Yang et al., 2023b; Wang et al., 2023b). $\mu_\theta(\mathbf{e}_n^t, \mathbf{c}, t)$ is the predicted mean from a network $f_\theta(\cdot)$:
 164 $\mu_\theta(\mathbf{e}_n^t, \mathbf{c}, t) = \frac{\sqrt{\bar{\alpha}_t}(1-\bar{\alpha}_{t-1})}{\sqrt{1-\bar{\alpha}_t}} \mathbf{e}_n^t + \frac{\sqrt{\bar{\alpha}_{t-1}}(1-\alpha_t)}{1-\bar{\alpha}_t} f_\theta(\mathbf{e}_n^t, \mathbf{c}, t)$. In DM-based recommendation methods,
 165 f_θ is generally implemented as an MLP for efficiency.
 166

167 The denoising process is guided by a preference condition \mathbf{c} constructed from the context items
 168 ($\{\mathbf{e}_1, \dots, \mathbf{e}_{n-1}\}$) using a sequence encoder (e.g., Transformer (Kang & McAuley, 2018), GRU
 169 (Hidasi et al., 2015)). This condition \mathbf{c} represents users' overall preference.
 170

171 **Optimization.** The core of DM-based sequential recommendation is to optimize the conditional
 172 data generation distribution $p_\theta(\mathbf{e}_n^0 | \mathbf{c})$, which is performed by optimizing the variational bound on
 173 negative log likelihood as follows:
 174

$$\mathbb{E}[-\log p_\theta(\mathbf{e}_n^0 | \mathbf{c})] \leq \mathbb{E}_q \left[-\log \frac{p_\theta(\mathbf{e}_n^{0:T} | \mathbf{c})}{q(\mathbf{e}_n^{1:T} | \mathbf{e}_n^0)} \right] := \mathcal{L}. \quad (3)$$

178 3 THE DISCO MODEL

180 In this section, we first introduce our disentangled diffusion model (Section 3.1) followed by the
 181 projection of diffusion targets into a credible subspace (Section 3.2). These two components jointly
 182 enable the learning of credible conditions and credible diffusion targets (i.e., two essential elements
 183 in diffusion models) to guide the model toward credible generation. Subsequently, to address the
 184 more realistic scenario where only a limited portion of content items are labeled with credibility
 185 information, we propose a progressive enhancement mechanism for the credible subspace (Section
 186 3.3). Thereafter, we present the overall optimization objective of our proposed model, which in-
 187 tegrates a content disentanglement term and a preference contrast term to simultaneously enhance
 188 recommendation credibility and accuracy (Section 3.4). Finally, we detail the credible generation
 189 and recommendation process after training (Section 3.5). All components are interlocked to con-
 190 struct a unified diffusion-based framework for accurate and credible content recommendation under
 191 limited credibility supervision. The pseudo-codes of our model are provided in Algorithms 1, 2, 3.
 192

193 3.1 DISENTANGLED DIFFUSION MODEL

195 Our disentangled diffusion model is built upon two objectives: (1) generating item embeddings that
 196 reflect users' genuine preferences; and (2) reducing the negative influence of uncredible content
 197 on the item embedding generation process. To achieve these objectives, we guide DM to generate
 198 the item embeddings using the preference-related condition while discouraging the guidance by
 199 uncredible content-related condition.
 200

201 To achieve this, we first introduce two content learners to extract user preference signals and uncred-
 202 ible content signals from items' embeddings. To ensure model simplicity and computational effi-
 203 ciency, both learners are implemented using MLP architectures. Formally, the preference-aware em-
 204 bedding \mathbf{e}^{pre} and the uncredible content-aware embedding \mathbf{e}^{unc} are obtained via $\mathbf{e}^{pre} = \text{MLP}_{pre}(\mathbf{e})$ and
 205 $\mathbf{e}^{unc} = \text{MLP}_{unc}(\mathbf{e})$, respectively. Accordingly, the context items in a user's interaction se-
 206 quence can be transformed into two separate sequences: the preference-related sequence $s^{pre} =$
 207 $\{\mathbf{e}_1^{pre}, \dots, \mathbf{e}_{n-1}^{pre}\}$ and the uncredible content-related sequence $s^{unc} = \{\mathbf{e}_1^{unc}, \dots, \mathbf{e}_{n-1}^{unc}\}$.
 208

209 Thereafter, we construct preference-related and uncredible content-related conditions from corre-
 210 sponding embedding sequences through a Transformer: $\mathbf{c}^{pre} = \text{Transformer}(\{\mathbf{e}_1^{pre}, \dots, \mathbf{e}_{n-1}^{pre}\})$
 211 and $\mathbf{c}^{unc} = \text{Transformer}(\{\mathbf{e}_1^{unc}, \dots, \mathbf{e}_{n-1}^{unc}\})$. We employ the same Transformer architecture with
 212 (Kang & McAuley, 2018; Yang et al., 2023b). However, applying the Transformer twice is com-
 213 putationally expensive. Therefore, we replace the Transformer with mean pooling to construct un-
 214 credible content-related condition (i.e., $\mathbf{c}^{unc} = \text{Mean}(\{\mathbf{e}_1^{unc}, \dots, \mathbf{e}_{n-1}^{unc}\})$), since content credibility
 215 does not exhibit temporal dependencies.
 216

217 After constructing the two conditions, Disco is optimized by jointly encouraging generation guided
 218 by preference-related condition \mathbf{c}^{pre} and discouraging generation guided by uncredible content-
 219 related condition \mathbf{c}^{unc} . Specifically, it minimizes the variational bound on the target item \mathbf{e}_n when
 220

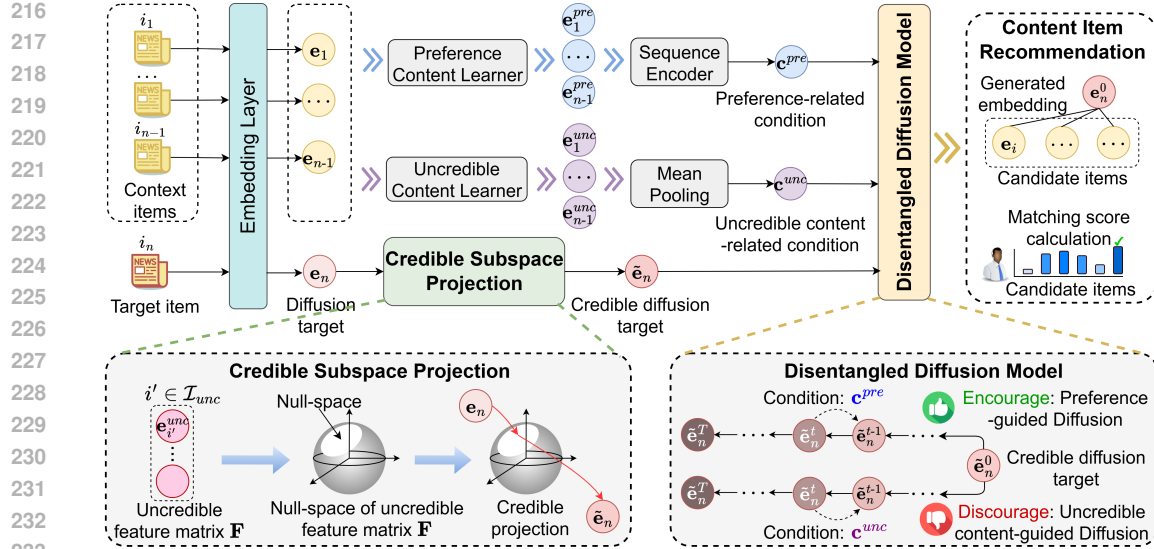


Figure 2: The overall framework of **Disco**. For simplicity and ease of understanding, the progressive enhancement of the credible subspace is not shown in the figure.

conditioned on \mathbf{c}^{pre} , while maximizing the variational bound when conditioned on \mathbf{c}^{unc} :

$$\theta^* = \arg \min_{\theta} \mathbb{E}_q \left[-\log \frac{p_{\theta}(\mathbf{e}_n^{0:T} | \mathbf{c}^{pre})}{q(\mathbf{e}_n^{0:T} | \mathbf{e}_n^0)} \right] - \mathbb{E}_q \left[-\log \frac{p_{\theta}(\mathbf{e}_n^{0:T} | \mathbf{c}^{unc})}{q(\mathbf{e}_n^{0:T} | \mathbf{e}_n^0)} \right]. \quad (4)$$

By employing this training objective, DM can naturally disentangle the two types of information without requiring additional components to explicitly enforce the separation. Importantly, we do not use \mathbf{e}_n^{pre} or \mathbf{e}_n^{unc} as diffusion targets. Otherwise, disentanglement would be ineffective because the diffusion condition and target would lie in the same space, lacking a meaningful disentanglement direction. Our ablation study in Section 4.3 further confirms this, showing that replacing \mathbf{e}_n with \mathbf{e}_n^{pre} or \mathbf{e}_n^{unc} significantly deteriorates recommendation performance.

The training objective in Equation 4 can be reformulated as the following loss:

$$\mathcal{L} = \mathbb{E}_{\mathbf{e}_n^0, \mathbf{c}^{pre}, t} [\|\mathbf{e}_n^0 - f_{\theta}(\mathbf{e}_n^t, \mathbf{c}^{pre}, t)\|_2^2] - \mathbb{E}_{\mathbf{e}_n^0, \mathbf{c}^{unc}, t} [\|\mathbf{e}_n^0 - f_{\theta}(\mathbf{e}_n^t, \mathbf{c}^{unc}, t)\|_2^2]. \quad (5)$$

The detailed derivation is provided in the Appendix D. However, directly training the model with this loss can lead to severe instability. Specifically, the second term may converge to an extremely small value, causing the model to predominantly optimize this term while neglecting the first term. To address this, inspired by (Liu et al., 2025a), we replace the MSE loss with a cosine loss:

$$\mathcal{L} = \mathbb{E}_{\mathbf{e}_n^0, \mathbf{c}^{pre}, t} [S(\mathbf{e}_n^0, f_{\theta}(\mathbf{e}_n^t, \mathbf{c}^{pre}, t))] - \mathbb{E}_{\mathbf{e}_n^0, \mathbf{c}^{unc}, t} [S(\mathbf{e}_n^0, f_{\theta}(\mathbf{e}_n^t, \mathbf{c}^{unc}, t))], \quad (6)$$

where $S(\cdot, \cdot) = (1 - \cos(\cdot, \cdot))^2$ and $\cos(\cdot, \cdot)$ is the cosine similarity of two embeddings. This loss preserves the same optimization direction as that in Equation 5, while its values remain within a stable range, thereby improving the stability of model training.

3.2 CREDIBLE SUBSPACE PROJECTION

The last item in a user’s interaction sequence may also be an uncredible item, leading to an uncredible diffusion target. In such cases, optimizing Equation 6 might still be suboptimal for mitigating uncredible content. To address this, we design a credible subspace projection operation, which projects the diffusion target into the credible subspace to suppress uncredible content.

To achieve this, we first construct an uncredible feature matrix $\mathbf{F} \in \mathbb{R}^{|\mathcal{I}_{unc}| \times d}$ by stacking the uncredible content embeddings of all uncredible items, i.e., $\{\mathbf{e}_i^{unc} | i \in \mathcal{I}_{unc}\}$, where \mathcal{I}_{unc} is the set of uncredible items and d is the embedding size. The credible subspace projection is then performed by projecting the diffusion target into the null space of \mathbf{F} , which serves as a subspace that maximally

270 excludes uncredible content. Following prior work on null-space projection (Fang et al., 2025; Wang
 271 et al., 2021a; Hu et al., 2025), we apply Singular Value Decomposition (SVD) on \mathbf{F}^\top :
 272

$$273 \quad \{\mathbf{U}, \mathbf{\Lambda}, \mathbf{V}\} = \text{SVD}(\mathbf{F}^\top), \quad (7)$$

275 where each column of left singular matrix \mathbf{U} is an orthogonal basis of \mathbf{F}^\top . \mathbf{V} denotes the right
 276 singular matrix. $\mathbf{\Lambda}$ contains the corresponding singular values, which indicate the magnitude of
 277 uncredible information encoded by the orthogonal basis in \mathbf{U} . A higher singular value corresponds
 278 to a orthogonal basis that is denser in uncredible information. Accordingly, we remove the submatrix
 279 \mathbf{U}_1 in \mathbf{U} whose singular values exceed a predefined threshold. The remaining submatrix, \mathbf{U}_2 ,
 280 consists only of orthogonal basis containing sparse or no uncredible information. The diffusion
 281 target is subsequently projected into the null space of \mathbf{F} using the following operation:
 282

$$282 \quad \tilde{\mathbf{e}}_n = \mathbf{e}_n \mathbf{U}_2 \mathbf{U}_2^\top, \quad (8)$$

284 where $\tilde{\mathbf{e}}_n$ is the credible diffusion target. To preserve the useful information contained in the original
 285 target item embedding \mathbf{e}_n , we adopt a residual connection to combine it with the projected embed-
 286 ding, yielding the responsible diffusion target as: $\tilde{\mathbf{e}}_n = (\tilde{\mathbf{e}}_n + \mathbf{e}_n)/2$. This credible diffusion target
 287 is then used to replace the original target in the diffusion loss, as defined in Equation 6:
 288

$$288 \quad \mathcal{L} = \mathbb{E}_{\tilde{\mathbf{e}}_n^0, \mathbf{c}^{pre}, t} [S(\tilde{\mathbf{e}}_n^0, f_\theta(\tilde{\mathbf{e}}_n^t, \mathbf{c}^{pre}, t))] - \mathbb{E}_{\tilde{\mathbf{e}}_n^0, \mathbf{c}^{unc}, t} [S(\tilde{\mathbf{e}}_n^0, f_\theta(\tilde{\mathbf{e}}_n^t, \mathbf{c}^{unc}, t))], \quad (9)$$

290 where $\tilde{\mathbf{e}}_n^0 = \tilde{\mathbf{e}}_n$. Training the model with this loss further enhances the credibility of recom-
 291 mendation generation by projecting the diffusion target into a more credible subspace.
 292

293 3.3 PROGRESSIVE ENHANCEMENT OF CREDIBLE PROJECTION

295 Owing to the second challenge mentioned in the introduction, the uncredible feature matrix \mathbf{F} may
 296 capture only a limited set of uncredible features, leading to an incomplete credible subspace projec-
 297 tion. To address this, we propose a progressive enhancement strategy for credible projection.
 298

299 Let \mathcal{I}_{unc} denote the set of items already labeled as uncredible content, and the remaining items
 300 in $\mathcal{I} \setminus \mathcal{I}_{unc}$ have uncertain labels. Actually, there is still a proportion of items in $\mathcal{I} \setminus \mathcal{I}_{unc}$ that
 301 are uncredible items but are not verified. In real-world scenarios, uncredible content often exhibits
 302 shared features. For instance, fake news articles tend to use emotionally charged or sensational
 303 headlines, such as those written in all capital letters¹. In light of this, we try to detect the potential
 304 uncredible items by calculating the uncredible degree of items in $\mathcal{I} \setminus \mathcal{I}_{unc}$:
 305

$$305 \quad \text{UD}(i) = \frac{1}{|\mathcal{I}_{unc}|} \sum_{i' \in \mathcal{I}_{unc}} \cos(\mathbf{e}_i^{unc}, \mathbf{e}_{i'}^{unc}), \quad (10)$$

308 where \mathbf{e}_i^{unc} and $\mathbf{e}_{i'}^{unc}$ are uncredible content embeddings of item i in $\mathcal{I} \setminus \mathcal{I}_{unc}$ and item i' in \mathcal{I}_{unc} .
 309 $\cos(\cdot, \cdot)$ calculates the cosine similarity between two embeddings. $\text{UD}(i)$ represents the uncredible
 310 degree of item i , quantifying the likelihood that item i in $\mathcal{I} \setminus \mathcal{I}_{unc}$ is an uncredible item. Items with
 311 the highest uncredible degrees are selected as potential uncredible items.
 312

313 At the early stages of training, the disentangled diffusion model is not fully trained, resulting in less
 314 accurate estimates of uncredible degrees. As training goes on, the model’s capability improves.
 315 Therefore, instead of using a fixed selection ratio, we propose a progressive selection strategy.
 316 Specifically, we predefine a maximum selection ratio γ and linearly increase the selection ratio
 317 from zero to γ after m training iterations. Consequently, the selection ratio at the j -th training it-
 318 eration is given by $\text{ratio}(j) = \min(\gamma, \frac{j}{m}\gamma)$. After calculating the current selection ratio, the top
 319 $\lfloor |\mathcal{I} \setminus \mathcal{I}_{unc}| \cdot \text{ratio}(j) \rfloor$ items in $\mathcal{I} \setminus \mathcal{I}_{unc}$ with the highest uncredible degrees are selected as the
 320 potential uncredible items and added to the set \mathcal{I}_{unc} . Subsequently, the uncredible feature matrix \mathbf{F}
 321 is updated based on the expanded set \mathcal{I}_{unc} . This update enhances the comprehensiveness of the null
 322 space of constructed uncredible content features, reduces residual uncredible features, and enables
 323 the diffusion target to be projected into a more credible subspace.

¹<https://techcrunch.com/2017/04/06/facebook-puts-link-to-10-tips-for-spotting-false-news-atop-feed/>

324 3.4 OVERALL OPTIMIZATION OBJECTIVE OF DISCO
325

326 The optimization loss in Equation 9 primarily addresses two objectives: capturing a user’s positive
327 preference (i.e., the target item) and enforcing content disentanglement. However, in RSs, modeling
328 a user’s negative preference is also crucial, as it enables the model to understand which types of
329 items users are not interested in. To incorporate this objective and further enhance recommendation
330 accuracy, we formulate the final version of our diffusion loss with an additional preference contrast
331 term by enlarging the distance between positive and negative preference:

$$\begin{aligned} \mathcal{L}_{\text{Disco}} = & \underbrace{S(\tilde{\mathbf{e}}_n^0, f_{\theta}(\tilde{\mathbf{e}}_n^t, \mathbf{c}^{\text{pre}}, t)) - S(\tilde{\mathbf{e}}_n^0, f_{\theta}(\tilde{\mathbf{e}}_n^t, \mathbf{c}^{\text{unc}}, t))}_{\text{Content disentanglement}} \\ & + \underbrace{w(S(\tilde{\mathbf{e}}_n^0, f_{\theta}(\tilde{\mathbf{e}}_n^t, \mathbf{c}^{\text{pre}}, t)) - S(\mathbf{e}_{\text{neg}}^0, f_{\theta}(\mathbf{e}_{\text{neg}}^t, \mathbf{c}^{\text{pre}}, t)))}_{\text{Preference contrast}}, \end{aligned} \quad (11)$$

332 where $\mathbf{e}_{\text{neg}}^0 = \mathbf{e}_{\text{neg}}$ is the embedding of a sampled negative preference item (i.e., an item that a
333 user has not interacted with). w is a hyperparameter controlling the contribution of each term, and
334 $t \sim U(0, T)$. For simplicity, we omit the expectation notation. The second term encourages the
335 diffusion model to generate items reflecting users’ positive preferences rather than negative prefer-
336 ences. Although computing this loss requires multiple forward passes through f_{θ} , the computational
337 overhead remains minimal, as f_{θ} is implemented as an MLP, which is time-efficient. Moreover, since
338 all components share a single f_{θ} network, no additional memory consumption is required.

346 3.5 CREDIBLE GENERATION AND CONTENT RECOMMENDATION
347

348 In this section, we describe the generation/inference process of Disco.

349 Following the generation paradigm of Denoising Diffusion Probabilistic Models (Ho et al., 2020),
350 the one-step generation procedure is defined as follows:

$$\mathbf{e}_n^{t-1} = \frac{\sqrt{\bar{\alpha}_{t-1}}(1 - \alpha_t)}{1 - \alpha_t} f_{\theta}(\mathbf{e}_n^t, \mathbf{c}^{\text{pre}}, t) + \frac{\sqrt{\alpha_t}(1 - \bar{\alpha}_{t-1})}{1 - \bar{\alpha}_t} \mathbf{e}_n^t + \sqrt{\frac{1 - \bar{\alpha}_{t-1}}{1 - \bar{\alpha}_t}(1 - \alpha_t)} \boldsymbol{\epsilon}. \quad (12)$$

351 The generation step begins with $\mathbf{e}_n^T \sim \mathcal{N}(\mathbf{0}, \mathbf{I})$. We employ preference-related condition \mathbf{c}^{pre} to
352 guide the generation, ensuring the generated embeddings capture users’ genuine preferences. This
353 approach prevents the generated embedding from incorporating uncredible content features, even
354 if users have previously interacted with uncredible items, thereby enhancing the credibility of the
355 generation. To improve efficiency, we adopt the DDIM sampling strategy (Song et al., 2021).

356 The generated embedding \mathbf{e}_n^0 represents the user’s predicted future preference. It is then used to
357 compute matching scores with candidate items: $\hat{y}_i = \mathbf{e}_n^0 \cdot \mathbf{e}_i^{\top}$, where \mathbf{e}_i is the embedding of candidate
358 item i . The top-K items with the highest matching scores are subsequently recommended to the user.

365 **Discussion: Comparison between Disco and other DM-based methods.**
366

- 367 • **Model architecture:** DreamRec Yang et al. (2023b), DiffuRec Li et al. (2023), and PreferDiff Liu
368 et al. (2025a) all adopt a single-channel diffusion architecture, in which a single condition is used
369 to guide the generation of the target item. In contrast, Disco employs a disentangled diffusion
370 architecture with dual channels, leveraging two conditions to guide the generation. This design
371 plays a crucial role in separating preference-related information from uncredible content signals.
- 372 • **Objective formulation:** DreamRec uses the standard ELBO objective for diffusion models,
373 whereas PreferDiff adopts a variant ELBO combined with a Bayesian Personalized Ranking
374 (BPR) loss. DiffuRec instead uses a cross-entropy (CE) objective, essentially turning a gener-
375 ative diffusion model into a discriminative one. By contrast, our model also belongs to a variant
376 of the ELBO, but one specifically designed to achieve both accurate and credible generation—an
377 ability that DreamRec, DiffuRec, and PreferDiff do not possess.

378 4 EXPERIMENTS
379380 4.1 EXPERIMENTAL SETUP
381

382 **Datasets.** We evaluate our method on three datasets: PolitiFact, GossipCop and MHMisinfo. The
383 PolitiFact and GossipCop datasets are derived from FakeNewsNet repository² (Shu et al., 2020).
384 These datasets contain user-news interaction data, where fake news is treated as uncredible content
385 items. Our task requires user-item interaction sequences together with credibility labels indicating
386 whether the items are credible items or not. To the best of our knowledge, these three datasets are the
387 only publicly available datasets that meet these requirements, which can be used in our experiments.
388 MHMisinfo is collected from a video-based mental health misinformation dataset³ (Nguyen et al.,
389 2025). This dataset contains users' interaction sequence with videos and the videos containing
390 misinformation are uncredible items. Since this dataset does not provide video metadata but only
391 textual descriptions, we use the textual descriptions as the item content. A detailed description of
392 these datasets is provided in the Appendix B.1.
393

394 **Baselines.** To evaluate the effectiveness of *Disco*, we compare it with four categories of sequential
395 recommendation methods: (1) **Traditional methods**, including GRU4Rec (Hidasi et al., 2015),
396 SASRec (Kang & McAuley, 2018), Bert4Rec (Sun et al., 2019), and LRURec (Yue et al., 2024); (2)
397 **Contrastive learning-based methods**, including CL4SRec (Xie et al., 2022) and ContraRec (Wang
398 et al., 2023a); (3) **Credible recommendation methods**, including Rec4Mit (Wang et al., 2022),
399 HDInt (Wang et al., 2024a), and PRISM (Ma et al., 2025); (4) **DM-based methods**, including
400 DreamRec (Yang et al., 2023b), DiffuRec (Li et al., 2023), PRISM (Ma et al., 2025), PreferDiff (Liu
401 et al., 2025a). The details of these methods are provided in the Appendix B.2.
402

403 **Evaluation Metrics.** We evaluate model performance using three types of metrics: accuracy-
404 oriented metrics such as HR@K and NDCG@K, a credibility-oriented metric CR@K (i.e., credible
405 rate), and a combined metric HC@K that integrates HR@K and CR@K. We follow the standard top-
406 K evaluation protocol with $K = 5, 10$, as commonly adopted in sequential recommendation tasks
407 (Kang & McAuley, 2018). Specifically, CR@K, proposed by (Wang et al., 2022), measures the pro-
408 portion of credible content items in the top-K recommendation list, where a higher value indicates a
409 more credible output. The detailed definitions of these metrics are provided in Appendix B.3.
410

411 **Implementation Details.** During training, we assume that labels for 20% of randomly selected un-
412 credible items are available, simulating the sparsity of labeled data in real-world scenarios. For fair
413 comparison, we initialize each model's hyperparameters as suggested in the original papers and then
414 fine-tune them on our datasets to ensure their best performances are reported. The hyperparameter
415 w is tuned within $\{0.5, 1, 1.5, 2, 5\}$, and γ within $\{0.1, 0.2, 0.3, 0.4, 0.5\}$, while m is fixed at 10,000.
416 The threshold for constructing the null space is fixed at 3. Model parameters are optimized using
417 AdamW (Loshchilov & Hutter, 2017). Each method is run five times, and we report the average per-
418 formance along with the standard deviation. Additional implementation details and hyperparameter
419 settings are provided in the Appendix B.4.
420

421 4.2 OVERALL PERFORMANCE COMPARISON
422

423 From the results reported in Table 1, we have the following observations:

424 **Our proposed method, *Disco*, consistently outperforms competitive methods in both accu-
425 rate and credible content recommendation.** *Disco* achieves the best performance across all
426 datasets and metrics. These results indicate that *Disco* can effectively reduce the recommenda-
427 tions of uncredible content while maintaining high recommendation accuracy. This is enabled by
428 the disentangled diffusion model and the progressively enhanced credible subspace projection. Not-
429 ably, *Disco* excels in recommendation accuracy due to the incorporation of negative preference
430 modeling, thereby better modeling users' genuine preference.

431 **DM-based methods generally exhibit better recommendation accuracy than other approaches.**
432 Thanks to their strong ability to model complex distributions of user behaviors and item content,
433 as well as to capture the inherent uncertainty in user behaviors, DM-based methods consistently
434

²<https://github.com/KaiDMML/FakeNewsNet>

³<https://zenodo.org/records/13191247>

432
 433 Table 1: Overall performance comparison. The best performances are in **bold**, and the second-best
 434 performances are underlined. The standard deviation is present in the form of percentage (%).

Datasets	Methods	HR@5↑	HR@10↑	NDCG@5↑	NDCG@10↑	CR@5↑	CR@10↑	HC@5↑	HC@10↑
PolitiFact	GRU4Rec	0.2142 ±0.51	0.3390 ±0.64	0.1463 ±0.37	0.1863 ±0.41	0.9266 ±0.84	0.9122 ±0.76	0.2929 ±0.51	0.3889 ±0.51
	SASRec	0.2158 ±0.10	0.3519 ±0.18	0.1386 ±0.05	0.1823 ±0.10	0.9059 ±0.41	0.9028 ±0.39	0.2929 ±0.12	0.3955 ±0.13
	LRURec	0.2168 ±0.14	0.3506 ±0.35	0.1443 ±0.06	0.1872 ±0.13	0.8976 ±0.20	0.8956 ±0.16	0.2924 ±0.14	0.3938 ±0.23
	Bert4Rec	0.2191 ±0.11	0.3473 ±0.16	0.1472 ±0.05	0.1883 ±0.08	0.9172 ±0.11	0.9045 ±0.15	0.2960 ±0.09	0.3929 ±0.13
	CL4SRec	0.2247 ±0.05	0.3527 ±0.17	0.1508 ±0.07	0.1919 ±0.05	0.9132 ±0.63	0.9027 ±0.67	0.3012 ±0.09	0.3960 ±0.14
	ContraRec	0.2241 ±0.25	0.3512 ±0.36	0.1508 ±0.11	0.1917 ±0.17	0.8803 ±2.67	0.8979 ±0.60	0.2969 ±0.35	0.3941 ±0.16
	Rec4Mit	0.2118 ±0.28	0.3449 ±0.40	0.1413 ±0.11	0.1840 ±0.15	0.8959 ±0.73	0.8925 ±0.59	0.2876 ±0.30	0.3891 ±0.25
	HDInt	0.2153 ±0.27	<u>0.3594 ±0.34</u>	0.1272 ±0.19	0.1734 ±0.21	0.8944 ±0.31	0.8946 ±0.36	0.2906 ±0.21	0.3985 ±0.18
	PRISM	0.1927 ±0.48	0.2758 ±0.27	0.1348 ±0.31	0.1615 ±0.25	0.9335 ±0.02	0.9172 ±0.21	0.2727 ±0.47	0.3446 ±0.26
	DreamRec	0.2416 ±0.88	0.3287 ±1.94	0.1767 ±1.70	0.2047 ±1.69	0.8620 ±3.24	0.8437 ±2.03	0.3054 ±1.42	0.3664 ±1.15
GossipCop	DiffuRec	<u>0.2606 ±1.21</u>	0.3558 ±1.69	<u>0.1894 ±0.92</u>	<u>0.2214 ±1.08</u>	0.9265 ±1.60	0.9153 ±0.76	<u>0.3334 ±0.81</u>	<u>0.4027 ±0.88</u>
	PreferDiff	0.2531 ±1.02	0.3554 ±0.52	0.1818 ±0.04	0.2147 ±0.86	0.8925 ±2.08	0.8981 ±2.34	0.3228 ±0.90	0.3968 ±0.75
	Disco	0.2678 ±0.53	0.3775 ±0.70	0.1983 ±0.17	0.2336 ±0.19	0.9823 ±0.34	0.9425 ±1.72	0.3466 ±0.50	0.4192 ±0.78
	<i>p</i> -values	$6.3e^{-2}$	$8.1e^{-3}$	$2.9e^{-2}$	$2.4e^{-2}$	$7.8e^{-4}$	$1.8e^{-2}$	$1.8e^{-2}$	$2.4e^{-2}$
	GRU4Rec	0.2226 ±2.44	0.3194 ±3.10	0.1466 ±1.83	0.1778 ±1.94	0.8864 ±1.80	0.8706 ±1.60	0.2957 ±2.61	0.3678 ±2.61
	SASRec	0.3078 ±0.19	0.4706 ±0.05	0.1607 ±0.19	0.2135 ±0.14	0.8743 ±1.87	0.8526 ±1.38	0.3612 ±0.49	0.4473 ±0.41
	LRURec	0.3316 ±0.18	0.5101 ±0.11	0.1697 ±0.12	0.2276 ±0.09	0.8544 ±2.39	0.8439 ±1.57	0.3732 ±0.52	0.4618 ±0.57
	Bert4Rec	0.2372 ±0.18	0.3711 ±0.18	0.1338 ±0.15	0.1770 ±0.14	0.8764 ±2.00	0.8587 ±0.74	0.3073 ±1.08	0.3984 ±0.12
	CL4SRec	0.2898 ±0.39	0.4100 ±0.45	0.1784 ±0.30	0.2174 ±0.30	0.8938 ±0.04	<u>0.8932 ±1.50</u>	0.3516 ±0.32	0.4275 ±0.39
	ContraRec	0.2848 ±0.14	0.4224 ±0.16	0.1574 ±0.15	0.2020 ±0.19	0.8754 ±2.06	0.8549 ±0.94	0.3450 ±0.39	0.4249 ±0.20
MHMisinfo	Rec4Mit	0.2775 ±1.73	0.4403 ±1.98	0.1606 ±1.26	0.2133 ±1.28	0.8979 ±0.62	0.8649 ±1.39	0.3427 ±1.57	0.4360 ±0.89
	HDInt	0.3407 ±0.15	0.5249 ±0.27	0.1748 ±0.09	0.2345 ±0.09	<u>0.8986 ±0.30</u>	0.8694 ±0.91	0.3875 ±0.14	0.4755 ±0.25
	PRISM	0.2948 ±0.33	0.3447 ±0.25	0.2301 ±0.30	0.2463 ±0.29	0.8806 ±3.09	0.8738 ±1.63	0.3531 ±0.70	0.3852 ±0.42
	DreamRec	0.4619 ±0.08	0.5501 ±0.13	0.3415 ±0.05	0.3704 ±0.07	0.8464 ±3.77	0.8339 ±1.93	0.4415 ±1.04	0.4742 ±0.61
	DiffuRec	0.4571 ±0.43	0.5008 ±0.65	<u>0.3887 ±0.23</u>	<u>0.4029 ±0.26</u>	0.8313 ±0.58	0.8157 ±0.45	0.4354 ±0.19	0.4495 ±0.24
	PreferDiff	<u>0.4969 ±0.05</u>	0.6022 ±0.07	0.3655 ±0.01	0.3999 ±0.02	0.8307 ±3.36	0.8228 ±2.76	<u>0.4523 ±1.14</u>	0.4887 ±0.88
	Disco	0.5236 ±0.80	0.6143 ±0.66	0.3996 ±0.91	0.4292 ±0.81	0.9277 ±0.28	0.9039 ±1.53	0.4918 ±0.40	0.5207 ±0.60
	<i>p</i> -values	$1.4e^{-3}$	$9.5e^{-3}$	$5.5e^{-2}$	$2.5e^{-3}$	$9.8e^{-5}$	$2.4e^{-1}$	$1.7e^{-3}$	$3.0e^{-3}$
	GRU4Rec	0.1151 ±4.47	0.1894 ±2.47	0.0760 ±4.43	0.0998 ±1.71	0.8380 ±2.68	0.8608 ±2.38	0.1803 ±2.18	0.2624 ±2.86
	SASRec	0.1485 ±0.39	0.2592 ±1.31	0.0826 ±0.26	0.1179 ±0.26	0.8839 ±1.24	0.8915 ±0.58	0.2190 ±0.56	0.3276 ±1.21
MHMisinfo	LRURec	0.1571 ±0.77	<u>0.2704 ±0.39</u>	0.0877 ±0.42	0.1268 ±0.39	0.8359 ±0.78	0.8818 ±0.76	0.2283 ±0.93	<u>0.3350 ±0.23</u>
	Bert4Rec	0.1391 ±0.70	0.2299 ±0.03	0.0847 ±0.44	0.1138 ±0.53	0.8162 ±0.75	0.8786 ±0.60	0.2074 ±0.92	0.3017 ±1.08
	CL4SRec	0.1734 ±0.50	0.2621 ±0.35	0.1101 ±0.30	0.1387 ±0.19	0.8577 ±0.43	0.9081 ±0.21	0.2469 ±0.57	0.3323 ±0.33
	ContraRec	0.1357 ±0.62	0.2258 ±0.58	0.0832 ±0.27	0.1122 ±0.28	0.8275 ±3.79	0.8760 ±2.45	0.2043 ±0.85	0.2980 ±0.74
	Rec4Mit	0.1460 ±1.00	0.2659 ±0.90	0.0886 ±0.60	0.1269 ±0.34	0.8424 ±0.76	0.9006 ±0.48	0.2166 ±1.24	0.3343 ±0.83
	HDInt	0.1471 ±0.40	0.2654 ±1.20	0.0852 ±0.25	0.1230 ±0.24	0.8306 ±0.38	0.8881 ±0.55	0.2168 ±0.61	0.3301 ±0.83
	PRISM	0.1700 ±1.31	0.2339 ±1.56	0.1181 ±0.62	0.1388 ±0.69	0.8398 ±3.91	0.8919 ±1.94	0.2418 ±1.39	0.3065 ±1.28
	DreamRec	0.1819 ±0.84	0.2426 ±0.67	0.1313 ±0.60	0.1509 ±0.54	<u>0.9002 ±2.94</u>	0.8952 ±3.06	0.2633 ±1.10	0.3176 ±0.87
	DiffuRec	0.1402 ±2.34	0.2095 ±2.77	0.0919 ±0.25	0.1142 ±1.97	0.8976 ±3.18	<u>0.9114 ±1.75</u>	0.2128 ±2.57	0.2861 ±2.49
	PreferDiff	<u>0.1974 ±0.72</u>	0.2620 ±0.59	<u>0.1389 ±0.54</u>	<u>0.1598 ±0.51</u>	0.8693 ±3.73	0.8874 ±2.31	<u>0.2713 ±0.85</u>	0.3294 ±0.80
	Disco	0.2215 ±0.89	0.2822 ±0.89	0.1580 ±0.69	0.1778 ±0.64	0.9305 ±0.82	0.9264 ±1.01	0.3000 ±0.97	0.3507 ±0.86
	<i>p</i> -values	$7.2e^{-3}$	$6.0e^{-2}$	$4.8e^{-3}$	$6.6e^{-3}$	$1.7e^{-2}$	$4.3e^{-3}$	$3.1e^{-3}$	$1.5e^{-2}$

469 outperform traditional recommendation approaches. Specifically, **Disco** consistently achieves the
 470 best performance, while DiffuRec and PreferDiff generally rank second across most cases. This
 471 observation aligns with prior works (Yang et al., 2023b; Liu et al., 2025a).

472 **Other methods focusing on credible content recommendation perform poorly under limited
 473 labeled data.** Although methods such as Rec4Mit, HDInt, and PRISM aim to mitigate the recom-
 474 mendation of uncredible content, they assume full access to labels for all uncredible items. This
 475 assumption does not hold in real-world scenarios, where a large portion of content items remain
 476 unverified. Consequently, these methods cannot achieve satisfactory uncredible content mitigation,
 477 as they rely on accurate and complete labeled data to train classifiers for detecting uncredible items.
 478 This limitation motivates our design of the progressively enhanced credible subspace projection,
 479 which has been empirically shown to effectively mitigate uncredible content.

481 4.3 ABLATION STUDY AND HYPERPARAMETER ANALYSIS

482 **Ablation Study.** In this section, we evaluate the effectiveness of each key component of **Disco**.
 483 We design six variants: (1) **w/o Dis**, which removes the disentanglement module (i.e., using origi-
 484 nal item embeddings for subsequent modeling); (2) **w/o CSP**, which removes the credible subspace
 485 projection; (3) **w/o PERS**, which removes the progressive enhancement of credible subspace; (4)

486

487

Table 2: Ablation study of Disco.

Methods	PolitiFact				GossipCop				MHMisinfo			
	HR@5	NDCG@5	CR@5	HC@5	HR@5	NDCG@5	CR@5	HC@5	HR@5	NDCG@5	CR@5	HC@5
Disco	0.2664	0.1975	0.9835	0.3455	0.5236	0.3996	0.9272	0.4918	0.2215	0.1580	0.9305	0.3000
w/o Dis	0.2273	0.1605	0.9121	0.3033	0.4984	0.3678	0.9193	0.4783	0.1910	0.1342	0.8654	0.2650
w/o CSP	0.2575	0.1809	0.9431	0.3331	0.5183	0.3898	0.9155	0.4860	0.2178	0.1548	0.9066	0.2942
w/o PERS	0.2651	0.1919	0.9423	0.3393	0.5147	0.3891	0.9267	0.4876	0.2103	0.1498	0.9113	0.2877
w/o PC	0.2637	0.1934	0.9677	0.3413	0.4643	0.3531	0.9316	0.4651	0.2006	0.1419	0.8708	0.2747
w/o CE	0.1034	0.0622	0.7600	0.1626	0.0005	0.0003	0.7600	0.0010	0.1613	0.1011	0.8000	0.2299
w/ DDT	0.2609	0.1899	0.9499	0.3368	0.4025	0.3190	0.9069	0.4265	0.2089	0.1458	0.8466	0.2797

494

w/o PC, which removes the preference contrast term in Equation 11; **(5) w/o CE**, which replaces cosine error with MSE in Equation 11; **(6) w/ DDT**, which utilizes disentangled embedding of target item as the diffusion target in Equation 4. As shown in Table 2, each component contributes positively. Specifically, removing the disentanglement module significantly harms model performance, highlighting that this module can effectively separate uncredible content and preserve users' preference-related information. Figure 3 also verifies that our designed disentangled diffusion model can effectively separate preference-related content and uncredible content. Both removing credible subspace projection and progressive enhancement of credible subspace significantly degrade Disco's recommendation credibility (i.e., CR@5). In addition, without the preference contrast term, the recommendation accuracy will deteriorate. In particular, if not replacing MSE loss with cosine error, Disco's performance will be degraded to a great extent, due to unstable training ([this issue is discussed in Appendix B.10 in detail](#)). Meanwhile, if using the disentangled item embedding as the diffusion target, Disco cannot obtain satisfactory recommendation performance, due to ineffective disentanglement.

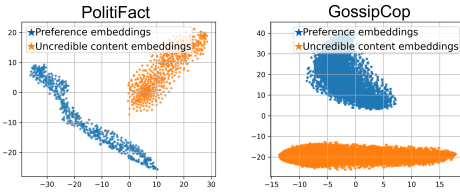


Figure 3: Disentanglement visualization.

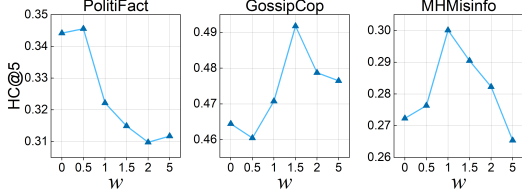


Figure 4: Effect of w on Disco.

515

516

Hyperparameter Analysis. The hyperparameter w controls the contribution of negative preference diffusion. As shown in Figure 4, Disco achieves the best performance when $w = 0.5$ on PolitiFact, $w = 1.5$ on GossipCop, and $w = 1$ on MHMisinfo. These results demonstrate the effectiveness of incorporating negative preference diffusion. However, continuously increasing the value of w leads to an imbalance between different training objectives, thereby deteriorating model performance. More analysis of hyperparameters are provided in Appendix B.5. [After analyzing the relationship between dataset statistics and the hyperparameter w, we found that the optimal value of w is proportional to the number of items in a dataset. The hyperparameter w controls the contribution of the preference-contrast term, which involves sampling negative items from the set of un-interacted items. When the number of items is larger, the sampled negative items represent a smaller portion of users' negative preferences. Therefore, a relatively larger w is needed to adequately learn users' negative preferences, thereby improving recommendation accuracy.](#)

529

530

5 CONCLUSIONS AND LIMITATIONS

531

532

In this paper, we proposed Disco, a model designed to steer DMs towards credible content recommendation. To this end, we first designed a disentangled diffusion model to separate uncredible content from the generation process. Considering the limited labeled data, a progressively enhanced credible subspace projection is proposed to make the diffusion training process more credible. However, similar to previous work (Liu et al., 2025a; Yang et al., 2023b), Disco also requires a relatively large embedding dimension to achieve strong performance. This inevitably leads to increased training time, which is a common limitation of current DM-based recommendation methods (Liu et al., 2025a). Future work could focus on designing DM-based models that maintain strong performance even under low-dimensional embeddings.

540 **Ethics Statement.** This paper aims to develop a diffusion model (DM)-based method for credible
 541 content recommendation. The goal of our approach is to serve societal good by mitigating the
 542 spread of uncredible content through recommender systems. We confirm that we do not anticipate
 543 any negative impacts and our work does not violate the ICLR code of ethics.

544 **Reproducibility Statement.** All results reported in this paper are fully reproducible. The pseudo
 545 codes of our model are provided in Algorithms 1, 2, and 3. The hyperparameter search space and
 546 experimental environment are discussed in Section B.4 and Table 4. We provide the code and data
 547 of our method at <https://anonymous.4open.science/r/Disco-4657/>.

549 **REFERENCES**

551 Zhuo Cai, Shoujin Wang, Victor W Chu, Usman Naseem, Yang Wang, and Fang Chen. Unleashing
 552 the potential of diffusion models towards diversified sequential recommendations. In *SIGIR*, pp.
 553 1476–1486, 2025.

554 Jianxin Chang, Chen Gao, Yu Zheng, Yiqun Hui, Yanan Niu, Yang Song, Depeng Jin, and Yong Li.
 555 Sequential recommendation with graph neural networks. In *SIGIR*, pp. 378–387, 2021.

557 Chong Chen, Fei Sun, Min Zhang, and Bolin Ding. Recommendation unlearning. In *WWW*, pp.
 558 2768–2777, 2022.

559 Junyoung Chung, Caglar Gulcehre, Kyunghyun Cho, and Yoshua Bengio. Empirical evaluation of
 560 gated recurrent neural networks on sequence modeling. In *NeurIPS Workshop on Deep Learning*,
 561 2014.

563 Ziqiang Cui, Haolun Wu, Bowei He, Ji Cheng, and Chen Ma. Context matters: Enhancing sequential
 564 recommendation with context-aware diffusion-based contrastive learning. In *CIKM*, pp. 404–414,
 565 2024a.

566 Ziqiang Cui, Haolun Wu, Bowei He, Ji Cheng, and Chen Ma. Diffusion-based contrastive learning
 567 for sequential recommendation. *arXiv preprint arXiv:2405.09369*, 2024b.

569 Yashar Deldjoo, Mehdi Elahi, Paolo Cremonesi, Franca Garzotto, Pietro Piazzolla, and Massimo
 570 Quadrana. Content-based video recommendation system based on stylistic visual features. *Journal
 571 on Data Semantics*, 5(2):99–113, 2016.

573 Yashar Deldjoo, Zhankui He, Julian McAuley, Anton Korikov, Scott Sanner, Arnaud Ramisa, René
 574 Vidal, Maheswaran Sathiamoorthy, Atoosa Kasirzadeh, and Silvia Milano. A review of modern
 575 recommender systems using generative models (gen-recsys). In *SIGKDD*, pp. 6448–6458, 2024.

576 Prafulla Dhariwal and Alexander Nichol. Diffusion models beat gans on image synthesis. volume 34,
 577 pp. 8780–8794, 2021.

579 Junfeng Fang, Houcheng Jiang, Kun Wang, Yunshan Ma, Jie Shi, Xiang Wang, Xiangnan He, and
 580 Tat-Seng Chua. Alphaedit: Null-space constrained knowledge editing for language models. In
 581 *ICLR*, 2025.

582 Miriam Fernandez, Alejandro Bellogín, and Iván Cantador. Analysing the effect of recommendation
 583 algorithms on the spread of misinformation. In *Proceedings of the ACM Web Science Conference*,
 584 pp. 159–169, 2024.

586 Mahesh Goyani and Neha Chaurasiya. A review of movie recommendation system: Limitations,
 587 survey and challenges. *ELCVIA. Electronic letters on computer vision and image analysis*, 19(3):
 588 0018–37, 2020.

589 Jesse Harte, Wouter Zorgdrager, Panos Louridas, Asterios Katsifodimos, Dietmar Jannach, and Mar-
 590 rios Fragkoulis. Leveraging large language models for sequential recommendation. In *RecSys*, pp.
 591 1096–1102, 2023.

593 Ruining He and Julian McAuley. Fusing similarity models with markov chains for sparse sequential
 594 recommendation. In *ICDM*, pp. 191–200, 2016.

594 Balázs Hidasi, Alexandros Karatzoglou, Linas Baltrunas, and Domonkos Tikk. Session-based rec-
 595 ommendations with recurrent neural networks. *arXiv preprint arXiv:1511.06939*, 2015.

596

597 Jonathan Ho and Tim Salimans. Classifier-free diffusion guidance. In *NeurIPS Workshop on Deep*
 598 *Generative Models and Downstream Applications*.

599

600 Jonathan Ho, Ajay Jain, and Pieter Abbeel. Denoising diffusion probabilistic models. volume 33,
 601 pp. 6840–6851, 2020.

602

603 Guoqing Hu, Zhengyi Yang, Zhibo Cai, An Zhang, and Xiang Wang. Generate and instanti-
 604 ate what you prefer: Text-guided diffusion for sequential recommendation. *arXiv preprint*
 605 *arXiv:2410.13428*, 2024.

606

607 Guoqing Hu, An Zhang, Shuo Liu, Zhibo Cai, Xun Yang, and Xiang Wang. Alphafuse: Learn id
 608 embeddings for sequential recommendation in null space of language embeddings. In *SIGIR*, pp.
 609 1614–1623, 2025.

610

611 Wang-Cheng Kang and Julian McAuley. Self-attentive sequential recommendation. In *ICDM*, pp.
 612 197–206, 2018.

613

614 Jin Li, Shoujin Wang, Qi Zhang, Shui Yu, and Fang Chen. Generating with fairness: A modality-
 615 diffused counterfactual framework for incomplete multimodal recommendations. In *WWW*, pp.
 616 2787–2798, 2025a.

617

618 Wuchao Li, Rui Huang, Haijun Zhao, Chi Liu, Kai Zheng, Qi Liu, Na Mou, Guorui Zhou, Defu
 619 Lian, Yang Song, et al. Dimerec: a unified framework for enhanced sequential recommendation
 620 via generative diffusion models. In *WSDM*, pp. 726–734, 2025b.

621

622 Xiang Li, John Thickstun, Ishaan Gulrajani, Percy S Liang, and Tatsunori B Hashimoto. Diffusion-
 623 lm improves controllable text generation. volume 35, pp. 4328–4343, 2022.

624

625 Zihao Li, Aixin Sun, and Chenliang Li. Diffurec: A diffusion model for sequential recommendation.
 626 *ACM Transactions on Information Systems*, 42(3):1–28, 2023.

627

628 Jianghao Lin, Jiaqi Liu, Jiachen Zhu, Yunjia Xi, Chengkai Liu, Yangtian Zhang, Yong Yu, and
 629 Weinan Zhang. A survey on diffusion models for recommender systems. *arXiv preprint*
 630 *arXiv:2409.05033*, 2024.

631

632 Qidong Liu, Fan Yan, Xiangyu Zhao, Zhaocheng Du, Huifeng Guo, Ruiming Tang, and Feng Tian.
 633 Diffusion augmentation for sequential recommendation. In *CIKM*, pp. 1576–1586, 2023.

634

635 Shuo Liu, An Zhang, Guoqing Hu, Hong Qian, and Tat-seng Chua. Preference diffusion for recom-
 636 mendation. In *ICLR*, 2025a.

637

638 Ziwei Liu, Qidong Liu, Yeqing Wang, Wanyu Wang, Pengyue Jia, Maolin Wang, Zitao Liu,
 639 Yi Chang, and Xiangyu Zhao. Sigma: Selective gated mamba for sequential recommendation. In
 640 *AAAI*, volume 39, pp. 12264–12272, 2025b.

641

642 Sahil Loomba, Alexandre De Figueiredo, Simon J Piatek, Kristen De Graaf, and Heidi J Larson.
 643 Measuring the impact of covid-19 vaccine misinformation on vaccination intent in the uk and
 644 usa. *Nature human behaviour*, 5(3):337–348, 2021.

645

646 Ilya Loshchilov and Frank Hutter. Decoupled weight decay regularization. *arXiv preprint*
 647 *arXiv:1711.05101*, 2017.

648

649 Justin Lovelace, Varsha Kishore, Chao Wan, Eliot Shekhtman, and Kilian Q Weinberger. Latent
 650 diffusion for language generation. volume 36, pp. 56998–57025, 2023.

651

652 Haokai Ma, Ruobing Xie, Lei Meng, Xin Chen, Xu Zhang, Leyu Lin, and Zhanhui Kang. Plug-in
 653 diffusion model for sequential recommendation. In *AAAI*, volume 38, pp. 8886–8894, 2024a.

654

655 Haokai Ma, Ruobing Xie, Lei Meng, Yimeng Yang, Xingwu Sun, and Zhanhui Kang. Seedrec:
 656 sememe-based diffusion for sequential recommendation. In *IJCAI*, pp. 1–9, 2024b.

648 Haokai Ma, Yimeng Yang, Lei Meng, Ruobing Xie, and Xiangxu Meng. Multimodal conditioned
 649 diffusion model for recommendation. In *WWW*, pp. 1733–1740, 2024c.
 650

651 Zihan Ma, Minnan Luo, Yiran Hao, Zhi Zeng, Xiangzheng Kong, and Jiahao Wang. Bridging inter-
 652 ests and truth: Towards mitigating fake news with personalized and truthful recommendations. In
 653 *SIGIR*, pp. 490–503, 2025.

654 Viet Cuong Nguyen, Mini Jain, Abhijat Chauhan, Heather Jamie Soled, Santiago Alvarez Lesmes,
 655 Zihang Li, Michael L Birnbaum, Sunny X Tang, Srijan Kumar, and Munmun De Choudhury.
 656 Supporters and skeptics: Llm-based analysis of engagement with mental health (mis) information
 657 content on video-sharing platforms. In *AAAI*, volume 19, pp. 1329–1345, 2025.
 658

659 Royal Pathak, Francesca Spezzano, and Maria Soledad Pera. Understanding the contribution of rec-
 660 ommendation algorithms on misinformation recommendation and misinformation dissemination
 661 on social networks. *ACM Transactions on the Web*, 17(4):1–26, 2023.

662 Tianhao Qi, Shancheng Fang, Yanze Wu, Hongtao Xie, Jiawei Liu, Lang Chen, Qian He, and Yong-
 663 dong Zhang. Deadiff: An efficient stylization diffusion model with disentangled representations.
 664 In *CVPR*, pp. 8693–8702, 2024.

665

666 Yuanpeng Qu and Hajime Nobuhara. Intent-aware diffusion with contrastive learning for sequential
 667 recommendation. In *SIGIR*, pp. 1552–1561, 2025.

668 Steffen Rendle, Christoph Freudenthaler, Zeno Gantner, and Lars Schmidt-Thieme. Bpr: Bayesian
 669 personalized ranking from implicit feedback. In *UAI*, pp. 452–461, 2009.

670

671 Leheng Sheng, An Zhang, Yi Zhang, Yuxin Chen, Xiang Wang, and Tat-Seng Chua. Language
 672 representations can be what recommenders need: Findings and potentials. In *ICLR*, 2025.

673

674 Kai Shu, Deepak Mahudeswaran, Suhang Wang, Dongwon Lee, and Huan Liu. Fakenewsnet: A
 675 data repository with news content, social context, and spatiotemporal information for studying
 676 fake news on social media. *Big data*, 8(3):171–188, 2020.

677 Jiaming Song, Chenlin Meng, and Stefano Ermon. Denoising diffusion implicit models. In *ICLR*,
 678 2021.

679

680 Fei Sun, Jun Liu, Jian Wu, Changhua Pei, Xiao Lin, Wenwu Ou, and Peng Jiang. Bert4rec: Sequenti-
 681 al recommendation with bidirectional encoder representations from transformer. In *CIKM*, pp.
 682 1441–1450, 2019.

683 Jiaxi Tang and Ke Wang. Personalized top-n sequential recommendation via convolutional sequence
 684 embedding. In *WSDM*, pp. 565–573, 2018.

685

686 Hugo Touvron, Louis Martin, Kevin Stone, Peter Albert, Amjad Almahairi, Yasmine Babaei, Niko-
 687 lay Bashlykov, Soumya Batra, Prajjwal Bhargava, Shruti Bhosale, et al. Llama 2: Open founda-
 688 tion and fine-tuned chat models. *arXiv preprint arXiv:2307.09288*, 2023.

689

690 Ashish Vaswani, Noam Shazeer, Niki Parmar, Jakob Uszkoreit, Llion Jones, Aidan N Gomez,
 691 Łukasz Kaiser, and Illia Polosukhin. Attention is all you need. *NeurIPS*, 30, 2017.

692

693 Chenyang Wang, Weizhi Ma, Chong Chen, Min Zhang, Yiqun Liu, and Shaoping Ma. Sequential
 694 recommendation with multiple contrast signals. *ACM Transactions on Information Systems*, 41
 (1):1–27, 2023a.

695

696 Shipeng Wang, Xiaorong Li, Jian Sun, and Zongben Xu. Training networks in null space of feature
 697 covariance for continual learning. In *CVPR*, pp. 184–193, 2021a.

698

699 Shoujin Wang, Liang Hu, Yan Wang, Longbing Cao, Quan Z. Sheng, and Mehmet Orgun. Sequential
 700 recommender systems: Challenges, progress and prospects. In *IJCAI*, 2019.

701 Shoujin Wang, Longbing Cao, Yan Wang, Quan Z. Sheng, Mehmet A. Orgun, and Defu Lian. A
 702 survey on session-based recommender systems. *ACM Computing Surveys*, 54(7):1–38, 2021b.

702 Shoujin Wang, Xiaofei Xu, Xiuzhen Zhang, Yan Wang, and Wenzhuo Song. Veracity-aware and
 703 event-driven personalized news recommendation for fake news mitigation. In *WWW*, pp. 3673–
 704 3684, 2022.

705 Shoujin Wang, Wentao Wang, Xiuzhen Zhang, Yan Wang, Huan Liu, and Fang Chen. A hierarchical
 706 and disentangling interest learning framework for unbiased and true news recommendation. In
 707 *SIGKDD*, pp. 3200–3211, 2024a.

708 Wenjie Wang, Yiyan Xu, Fuli Feng, Xinyu Lin, Xiangnan He, and Tat-Seng Chua. Diffusion re-
 709 commender model. In *SIGIR*, pp. 832–841, 2023b.

710 Yu Wang, Zhiwei Liu, Liangwei Yang, and Philip S Yu. Conditional denoising diffusion for se-
 711 quential recommendation. In *PAKDD*, pp. 156–169, 2024b.

712 Zhizhong Wang, Lei Zhao, and Wei Xing. Stylediffusion: Controllable disentangled style transfer
 713 via diffusion models. In *ICCV*, pp. 7677–7689, 2023c.

714 Ting-Ruen Wei and Yi Fang. Diffusion models in recommendation systems: A survey. *arXiv*
 715 preprint [arXiv:2501.10548](https://arxiv.org/abs/2501.10548), 2025.

716 Chuhuan Wu, Fangzhao Wu, Yongfeng Huang, and Xing Xie. Personalized news recommendation:
 717 Methods and challenges. *ACM Transactions on Information Systems*, 41(1):1–50, 2023a.

718 Zihao Wu, Xin Wang, Hong Chen, Kaidong Li, Yi Han, Lifeng Sun, and Wenwu Zhu. Diff4rec: Se-
 719 quential recommendation with curriculum-scheduled diffusion augmentation. In *MM*, pp. 9329–
 720 9335, 2023b.

721 Wenjia Xie, Rui Zhou, Hao Wang, Tingjia Shen, and Enhong Chen. Bridging user dynamics: Trans-
 722 forming sequential recommendations with schrödinger bridge and diffusion models. In *CIKM*,
 723 pp. 2618–2628, 2024.

724 Xu Xie, Fei Sun, Zhaoyang Liu, Shiwen Wu, Jinyang Gao, Jiandong Zhang, Bolin Ding, and Bin
 725 Cui. Contrastive learning for sequential recommendation. In *ICDM*, pp. 1259–1273, 2022.

726 Zhengyi Yang, Xiangnan He, Jizhi Zhang, Jiancan Wu, Xin Xin, Jiawei Chen, and Xiang Wang. A
 727 generic learning framework for sequential recommendation with distribution shifts. In *SIGIR*, pp.
 728 331–340, 2023a.

729 Zhengyi Yang, Jiancan Wu, Zhicai Wang, Xiang Wang, Yancheng Yuan, and Xiangnan He. Gen-
 730 erate what you prefer: Reshaping sequential recommendation via guided diffusion. In *NeurIPS*,
 731 volume 36, 2023b.

732 Ghim-Eng Yap, Xiao-Li Li, and Philip S Yu. Effective next-items recommendation via personalized
 733 sequential pattern mining. In *DASFAA*, pp. 48–64. Springer, 2012.

734 Zhenrui Yue, Yueqi Wang, Zhankui He, Huimin Zeng, Julian McAuley, and Dong Wang. Linear
 735 recurrent units for sequential recommendation. In *WSDM*, pp. 930–938, 2024.

736 Shuai Zhang, Yi Tay, Lina Yao, and Aixin Sun. Next item recommendation with self-attention.
 737 *arXiv* preprint [arXiv:1808.06414](https://arxiv.org/abs/1808.06414), 2018.

738 Yang Zhang, Zhiyu Hu, Yimeng Bai, Jiancan Wu, Qifan Wang, and Fuli Feng. Recommendation
 739 unlearning via influence function. *ACM Transactions on Recommender Systems*, 3(2):1–23, 2024.

740 Jujia Zhao, Wang Wenjie, Yiyan Xu, Teng Sun, Fuli Feng, and Tat-Seng Chua. Denoising diffusion
 741 recommender model. In *SIGIR*, pp. 1370–1379, 2024.

742

743

744

745

746

747

748

749

750

751

752

753

754

755

756 A RELATED WORK
757
758

759 Our content recommendation task follows the paradigm of sequential recommendation (SRec)
760 (Kang & McAuley, 2018; Wang et al., 2019). Accordingly, our work is closely aligned with the
761 research on sequential recommendation and diffusion model (DM)-based sequential recommenda-
762 tion. In this section, we review the studies on these two topics in detail.

763
764 A.1 SEQUENTIAL RECOMMENDATION
765

766 Sequential recommendation (SRec) has been widely studied in RSs, owing to the natural temporal
767 order of users' behaviors (Wang et al., 2019; 2021b). SRec can be technically divided into two
768 categories: traditional sequential models and deep learning-based models. Traditional sequential
769 models generally leverage sequential pattern mining (Yap et al., 2012) or Markov chain models
770 (He & McAuley, 2016) to model the item dependencies in users' interaction sequences. Traditional
771 sequential methods can only capture simple interaction patterns or short-term dependencies,
772 thereby cannot achieve satisfactory recommendation performance. To overcome these limitations,
773 deep learning-based sequential recommendation methods are proposed to model complex and long-
774 term dependencies in users' behaviors. Among this category, one research line focuses on designing
775 the effective sequence encoders and backbone networks to encode users' interaction sequence, in-
776 cluding GRU (Hidasi et al., 2015), CNNs (Tang & Wang, 2018), Transformer (Kang & McAuley,
777 2018), and Mamba (Liu et al., 2025b). Building upon these, another research line further introduces
778 advanced models, such as Graph Neural Networks (GNNs) (Chang et al., 2021) and generative
779 models (Deldjoo et al., 2024). Among them, generative models have recently attracted significant
780 attention. In particular, DMs Liu et al. (2025a) and large language models (LLMs) (Sheng et al.,
781 2025) have emerged as the two most prominent approaches. DM-based methods will be discussed in
782 detail in Section A.2. LLM-based methods focus on leveraging the open-world knowledge encoded
783 in LLMs to enhance sequential recommendation performance (Harte et al., 2023).

784
785 A.2 DIFFUSION MODELS FOR SEQUENTIAL RECOMMENDATION
786

787 In recent years, owing to the strong capability to model complex distributions of user behaviors
788 and item content, diffusion models (DMs) have been widely applied in recommendation scenarios
789 (Wei & Fang, 2025; Lin et al., 2024), including top-K recommendation (Wang et al., 2023b; Zhao
790 et al., 2024) and multimodal recommendation (Ma et al., 2024c; Li et al., 2025a). In SRec, DM-
791 based recommendation methods can be broadly categorized into two types: next item generation-
792 based methods, and data augmentation-based methods. The former generally employ sequence
793 encoders (e.g., GRU and Transformer) to encode users' context items into condition embeddings,
794 which then guide the generation of next items (Yang et al., 2023b; Liu et al., 2025a; Li et al.,
795 2025b; Cai et al., 2025; Hu et al., 2024; Li et al., 2025b; Ma et al., 2024b; Wang et al., 2024b;
796 Xie et al., 2024). For example, (Yang et al., 2023b; Liu et al., 2025a) utilize Transformer to learn
797 condition embeddings from users' historical interactions, which are then utilized to guide the next-
798 item generation process. The latter category leverages DMs to generate additional interaction data in
799 order to enrich users' interaction sequences and alleviate sequence sparsity. For instance, (Liu et al.,
800 2023; Ma et al., 2024a; Wu et al., 2023b) propose generating pseudo interaction sequences with
801 DMs to mitigate the sequence sparsity problem. Additionally, several methods integrate contrastive
802 learning with diffusion models to generate augmented views, thereby enhancing the training of DM-
803 based recommendation methods (Cui et al., 2024b;a; Qu & Nobuhara, 2025).

804 Although these methods have achieved remarkable success, they pose a significant risk of generating
805 uncredible content recommendations (e.g., fake news (Wang et al., 2022; 2024a; Ma et al., 2025),
806 misinformation (Pathak et al., 2023; Fernandez et al., 2024)), which can severely harm both user
807 experience and societal well-being. While (Ma et al., 2025) attempts to leverage DMs to mitigate
808 fake news, its effectiveness is limited under the challenge of scarce labeled data. This limitation moti-
809 vates us to steer DMs towards credible content recommendation while simultaneously addressing
the challenge of learning from only limited annotated data.

810 B MORE EXPERIMENTAL DETAILS
811812 B.1 DATASETS
813814 In our task setting, we require users’ chronological interaction sequences with content items, to-
815 gether with labels indicating whether each item contains uncredible content. However, only a lim-
816 ited number of public datasets fulfill these requirements. In this paper, we utilize three datasets:
817 PolitiFact, GossipCop, and MHMisinfo.818 The PolitiFact and GossipCop datasets are derived from the FakeNewsNet repository⁴ , which col-
819 lects data from two well-known fact-checking websites: PolitiFact and GossipCop. These datasets
820 provide user–news interaction sequences along with labels that indicate whether each news article
821 is fake or true. The MHMisinfo dataset is collected from a video-based mental health misinfor-
822 mation dataset⁵ , containing users’ interaction sequences with videos annotated by whether the videos
823 contain mental health misinformation. Although this dataset records user–video interactions, the
824 original video and image contents are not provided. Therefore, we represent the items using their
825 video descriptions instead of visual features.826 Given the high sparsity of these datasets, we adopt a data augmentation strategy following common
827 practice (Yang et al., 2023b;a). Specifically, for each user, we transform their interaction sequence
828 into multiple sub-sequences by treating each item as the target item and the items preceding it as
829 historical context. This transformation increases the number of user–item interaction sequences and
830 enriches the training data. The statistics of these datasets are reported in Table 3. After augmenta-
831 tion, the datasets have more sequences, thereby the recommendation performances of Rec4Mit and
832 HDInt are different from the results reported in (Wang et al., 2022) and (Wang et al., 2024a).833
834 Table 3: The statistics of the three used datasets after preprocessing.835

836 Datasets	837 PolitiFact	838 GossipCop	839 MHMisinfo
836 # Content items	837 616	838 9,529	839 3,160
836 # Credible content items	837 306	838 6,792	839 2,815
836 # Uncredible content items	837 310	838 2,737	839 345
836 # Training sequences	837 103,335	838 510,149	839 38,083
836 # Test sequences	837 21,490	838 68,002	839 8,060

841
842 B.2 BASELINE DESCRIPTIONS
843

844 In this section, we introduce the baseline methods used in our comparison.

845 **Traditional sequential recommendation methods:**
846847 • **GRU4Rec** (Hidasi et al., 2015) utilizes the Gated Recurrent Unit (GRU) to model the temporal
848 dependencies of items in users’ interaction sequences.
849 • **SASRec** (Kang & McAuley, 2018) employs the Transformer architecture to model the item de-
850 pendencies in users’ interaction sequences. This is one of the most representative sequential rec-
851 ommendation methods.
852 • **Bert4Rec** (Sun et al., 2019) replaces SASRec’s unidirectional Transformer with a bidirectional
853 Transformer architecture to model complex item dependencies. It also introduces a cloze task
854 paradigm for sequential recommendation.
855 • **LRU4Rec** (Yue et al., 2024) designs linear recurrent units for sequential recommendation. It
856 decomposes linear recurrence operations and proposes recursive parallelization, reducing model
857 size and enabling efficient parallel training.858
859 **Contrastive learning-based sequential recommendation methods:**
860861 • **CL4SRec** (Xie et al., 2022) uses contrastive learning to address the data sparsity problem in
862 sequential recommendation. It designs three sequence augmentation operations for contrastive863
864 ⁴<https://github.com/KaiDMML/FakeNewsNet>⁵<https://zenodo.org/records/13191247>

864 learning: item cropping, item masking, and item reordering. Transformer is used as the sequential
 865 encoder of CL4SRec.

866 • **ContraRec** (Wang et al., 2023a) proposes two types of contrastive perspectives to enhance the per-
 867 formance of contrastive learning-based sequential recommendation: context-target contrast and
 868 context-context contrast. Transformer is used as the sequential encoder of ContraRec.

870 **Sequential recommendation methods for mitigating uncredible content:**

872 • **Rec4Mit** (Wang et al., 2022) first utilizes a disentangler to extract event- and veracity-aware in-
 873 formation, respectively. Thereafter, the event embeddings are utilized to derive users’ genuine
 874 preferences and predict the next items users may be interested in.

875 • **HDInt** (Wang et al., 2024a). Similar to Rec4Mit, HDInt is also dedicated to mitigating fake news
 876 in recommender systems. HDInt also considers the political bias. We omit this part, since it
 877 requires additional data and the political bias is not considered in our task.

878 • **PRISM** (Ma et al., 2025) proposes a protection-enhanced news recommendation method based
 879 on interest-aware sequential modeling. It utilizes DMs’ controllable ability to learn user interest
 880 and mitigate fake news. However, it assumes all the labels of fake news are fully available, which
 881 does not hold in the real world. It is also a DM-based sequential recommendation method.

882 **DM-based recommendation methods:**

884 • **DreamRec** (Yang et al., 2023b) assumes that each user has an “oracle” item in mind and selects
 885 items that match his ideal item. It uses a Transformer to learn users’ preferences, which then serve
 886 as the condition for generating the oracle item for each user.

888 • **DiffuRec** (Li et al., 2023) employs a diffusion model to represent item embeddings in a distribu-
 889 tion space and then feeds the embeddings into an approximator to generate target item represen-
 890 tations. It argues that the standard objective function of DMs is unsuitable for recommendation
 891 tasks and uses cross-entropy loss to optimize model parameters.

892 • **PreferDiff** (Liu et al., 2025a) proposes a surrogate optimization objective which extend BPR
 893 recommendation loss (Rendle et al., 2009) to variational format. Meanwhile, this surrogate opti-
 894 mization objective can also be extended to multiple negative items.

895 **B.3 EVALUATION METRICS**

897 HR@K and NDCG@K are two commonly used metrics to evaluate the recommendation accuracy,
 898 thereby we do not make further introduction for them. Credible Rate (CR@K) is a metric to measure
 899 the credibility of a recommendation model. Specifically, it calculates the average rate of the credible
 900 content items in the recommendation lists:

$$902 \text{CR@K} = \frac{1}{|\mathcal{S}_{test}|} \sum_{s \in \mathcal{S}_{test}} \frac{K - |\mathcal{R}_s \cap \mathcal{I}_{unc}^{Ground-truth}|}{K}, \quad (13)$$

905 where \mathcal{S}_{test} is the test set of sequences. \mathcal{R}_s is the recommendation list for sequence s .
 $\mathcal{I}_{unc}^{Ground-truth}$ denotes the ground-truth set of uncredible items. $|\mathcal{R}_s \cap \mathcal{I}_{neg}^{Ground-truth}|$ calculates
 906 the number of uncredible items in the recommendation list. The higher value of CR@K means the
 907 better performance in delivering credible recommendations.

909 In addition, we test how our methods perform in terms of both accurate and credible recommenda-
 910 tions, we design a combined metric HC@K (i.e., combining HR@K and CR@K). Formally, HC@K
 911 is calculated as follows:

$$912 \text{HC@K} = \frac{2 \times \text{HR@K} \times (\text{CR@K}/2)}{\text{HR@K} + (\text{CR@K}/2)}. \quad (14)$$

914 This combined metric is inspired by the F1-score, which combines precision rate and recall rate.
 915 To note that, since the values of HR@K and CR@K are not on the same scale, we divide CR@K
 916 with a factor of 2 to rescale it into a similar value level with HR@K. This adjustment ensures a
 917 fair combination; otherwise, the metric with a much smaller magnitude would disproportionately
 dominate the combined score.

918 B.4 IMPLEMENTATION DETAILS
919

920 In this paper, we consider a more challenging and realistic scenario in which only a small proportion
921 of uncredible items are verified. To simulate this setting, we randomly select 20% of the uncredible
922 items with available labels during the training process, while the labels of the remaining items are
923 treated as unknown. It is similar to the semi-supervised setting. In contrast, during the testing stage,
924 all content labels are provided to enable an accurate evaluation.

925 The items in PolitiFact and GossipCop are news articles, and we use their textual descriptions as item
926 content. In MHMisinfo, although the items are videos, only textual descriptions are available; thus,
927 we can only rely on the textual descriptions for content representation. We encode these textual de-
928 scriptions into language embeddings using LLaMA2-7B (Touvron et al., 2023), and further project
929 them into a lower dimension through an MLP. Following (Liu et al., 2025a), we fix the transformed
930 embedding dimension at 3072 for all DM-based methods, as they exhibit strong performance only
931 with higher embedding sizes. For other methods, the embedding size is set to 64. We also exper-
932 imented with larger embedding sizes for these methods, but observed little or no performance gain,
933 and even performance drops for some methods, consistent with the findings in (Liu et al., 2025a).

934 In our implementation, we select Transformer as our sequence encoder. Following the standard
935 configuration (Vaswani et al., 2017), the Transformer architecture in our implementation includes
936 multi-head attention, position-wise feed-forward network, layer normalization, and dropout.

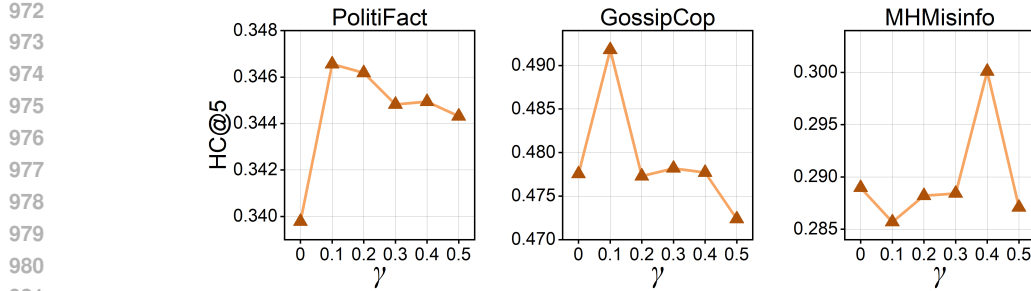
937 For our method `Disco`, the hyperparameter w is tuned within $\{0.5, 1, 1.5, 2, 5\}$. We fix m at
938 10,000 and tune γ within $\{0.1, 0.2, 0.3, 0.4, 0.5\}$ to control the maximum selection ratio as well as
939 the growth rate of the current selection ratio. The maximum number of diffusion steps is fixed at
940 2,000 and the DDIM step is set to 100, following the settings of (Liu et al., 2025a). For all DM-based
941 methods, we utilize a linear schedule for β_t in range $[0.0001, 0.02]$. In our implementation, we do
942 not use a classifier-free guidance (Ho & Salimans), since we found it does not influence much to the
943 performance of `Disco`. In our implementation, we found that the singular values in Λ are relatively
944 large; therefore, the threshold for constructing the null space of uncredible features is fixed at 3 for
945 all datasets in our experiments. We search learning rate in range $\{1e-5, 5e-5, 1e-4, 5e-4, 1e-3\}$. The
946 batch size is searched in $\{2048 \times 2^i\}_{i=0,1,2,3}$. The model parameters are initialized using normal
947 initialization and optimized by AdamW (Loshchilov & Hutter, 2017). The hyperparameter settings
948 of baseline methods are reported in Table 4. All experiments are conducted on an NVIDIA A40
949 GPU with 48 GB of memory. Each method is run five times, and we report the average performance
along with the standard deviation.

950
951 Table 4: The hyperparameter settings of baseline methods.
952

953 Methods	954 Hyperparameter searching space
955 GRU4Rec	lr~ $\{1e-2, 5e-2, 1e-3, 5e-3, 1e-4\}$, weight decay=0
956 SASRec	lr~ $\{1e-2, 5e-2, 1e-3, 5e-3, 1e-4\}$, weight decay=0
957 Bert4Rec	lr~ $\{1e-2, 5e-2, 1e-3, 5e-3, 1e-4\}$, weight decay=0, mask probability~ $\{0.2, 0.4, 0.6, 0.8\}$
958 LRURec	lr~ $\{1e-2, 5e-2, 1e-3, 5e-3, 1e-4\}$, weight decay=0, dropout rate~ $\{0.2, 0.4, 0.6, 0.8\}$
959 CL4SRec	lr~ $\{1e-2, 5e-2, 1e-3, 5e-3, 1e-4\}$, weight decay=0, mask/reorder/crop proportion~ $\{0.2, 0.4, 0.6, 0.8\}$, $\lambda \sim \{0.1, 0.3, \dots, 0.9\}$
960 ContraRec	lr~ $\{1e-2, 5e-2, 1e-3, 5e-3, 1e-4\}$, weight decay=0, mask/reorder/crop proportion~ $\{0.2, 0.4, 0.6, 0.8\}$, $\tau_1, \tau_2 \sim \{0.1, 0.2, \dots, 1\}$, $\gamma \sim \{0, 0.01, 0.1, 1, 5, 10\}$
961 Rec4Mit	lr~ $\{1e-2, 5e-2, 1e-3, 5e-3, 1e-4\}$, weight decay=0, $k \sim \{2, 4, \dots, 20\}$
962 HDInt	lr~ $\{1e-2, 5e-2, 1e-3, 5e-3, 1e-4\}$, weight decay=0, $\lambda \sim \{1, 2, \dots, 10\}$, $\gamma \sim \{2, 4, 6, 8, 10\}$
963 PRISM	lr~ $\{1e-2, 5e-2, 1e-3, 5e-3, 1e-4\}$, weight decay=0, $T \sim \{500, 1000, 1500, 2000\}$, $w \sim \{0, 2, 4, 6, 8\}$, $\lambda_{OT}, \lambda_c, \lambda_r, \lambda_{rec} \sim \{0.2, 0.4, 0.6, 0.8, 1\}$, embedding size~ $\{64, 128, 256, 512, 1024, 2048, 3072\}$
964 DreamRec	lr~ $\{1e-2, 5e-2, 1e-3, 5e-3, 1e-4\}$, weight decay=0, $T \sim \{500, 1000, 1500, 2000\}$, $w \sim \{0, 2, 4, 6, 8\}$, embedding size~ $\{64, 128, 256, 512, 1024, 2048, 3072\}$
965 DiffuRec	lr~ $\{1e-2, 5e-2, 1e-3, 5e-3, 1e-4\}$, weight decay=0, $T \sim \{16, 32, 64, 128\}$, $\delta=0.001$, embedding size~ $\{64, 128, 256, 512, 1024, 2048, 3072\}$
966 PreferDiff	lr~ $\{1e-2, 5e-2, 1e-3, 5e-3, 1e-4\}$, weight decay=0, $T \sim \{500, 1000, 1500, 2000\}$, $w \sim \{0, 2, 4, 6, 8\}$, $\lambda \sim \{0.2, 0.4, 0.6, 0.8\}$, embedding size~ $\{64, 128, 256, 512, 1024, 2048, 3072\}$

966 B.5 MORE HYPERPARAMETER EXPERIMENTS
967

968 The hyperparameter γ controls the selection ratio of potential uncredible items. We evaluate the
969 performance of `Disco` (using combined metric HC@5) under different values of γ in range $\{0.1,$
970 $0.2, 0.3, 0.4, 0.5\}$. As shown in Figure 5, `Disco` achieves the best performance when fixing $w =$
971 0.1 on PolitiFact and GossipCop, and $w = 0.4$ on MHMisinfo. Lower values prevent the model

Figure 5: Effect of γ on Disco.

from effectively capturing potentially uncredible items, while higher values may introduce excessive noise, both of which degrade model performance.

B.6 TIME EFFICIENCY ANALYSIS

We conduct experiments to evaluate the training and inference cost (in seconds) of our model `Disco` and four DM-based methods under the same batch size. As shown in Table 5, the training cost of `Disco` is relatively higher than `DreamRec` and `PreferDiff`, mainly due to our additional designs for credible content recommendation, including content disentanglement and credible subspace projection. This is acceptable due to the higher recommendation accuracy and credibility of our proposed method. Our training cost is much lower than that of `DiffuRec` and `PRISM`. As for inference cost, our proposed method `Disco` demonstrates the highest efficiency. This is because we adopt DDIM (Song et al., 2021) as our generation strategy, which is more efficient than the DDPM (Ho et al., 2020) paradigm employed by `DreamRec`, `DiffuRec` and `PRISM`. Even compared with `PreferDiff`, which also adopts DDIM, `Disco` also exhibits higher efficiency. It is because we do not employ classifier-free guidance in our implementation, since it has limited influence on our model while incurring additional time consumption. Although `Disco` requires disentangling item embeddings first in the inference stage, its inference cost remains comparable to `PreferDiff` on `GossipCop` dataset, which contain large number of items.

Table 5: Time cost (s) of different models on PolitiFact, GossipCop, and MHMisinfo.

Datasets	Time cost (s)	DreamRec	DiffuRec	PRISM	PreferDiff	Disco
PolitiFact	Training/epoch	9.4	74.8	25.3	11.3	12.6
	Inference	278.2	224.3	994.3	15.2	10.5
GossipCop	Training/epoch	43.3	376.9	137.6	58.8	73.1
	Inference	956.8	783.1	3223.6	127.9	133.5
MHMisinfo	Training/epoch	3.3	26.9	8.9	3.9	4.2
	Inference	107.6	87.1	372.9	8.7	7.7

B.7 DISCUSSION ON EMBEDDING DIMENSION

As pointed out in our paper, DM-based methods can only achieve strong performance when the embedding dimension is high. To demonstrate the necessity of using high embedding dimension (i.e., 3072) for all DM-based methods, we conducted experiments on DM-based methods when fixing embedding dimension to 64. The results are shown in Table 6:

As shown in Table 6, not only `Disco` but also other DM-based recommendation methods (`PRISM`, `DreamRec`, and `PreferDiff`) experience a substantial performance drop when the embedding size is reduced to 64. This observation is consistent with the findings reported in [1] and further validates the necessity of using high-dimensional embeddings in DM-based recommender systems.

Although a higher embedding dimension increases the per-epoch training time, it also provides the benefit of significantly faster convergence. In our revised manuscript, we include a figure illustrating the convergence curves of `Disco` and `SASRec`. As presented in Figure 6, `Disco` converges much

1026

1027

Table 6: Performance comparison under embedding dimension 64 for DM-based methods.

1028

1029

Methods	HR@5	HR@10	NDCG@5	NDCG@10	CR@5	CR@10	HC@5	HC@10
PolitiFact								
GRU4Rec	0.2142	0.3390	0.1463	0.1863	0.9266	0.9122	0.2929	0.3889
SASRec	0.2158	0.3519	0.1386	0.1823	0.9059	0.9028	0.2923	0.3955
Bert4Rec	0.2191	0.3473	0.1472	0.1883	0.9127	0.9045	0.2960	0.3929
CL4SRec	0.2247	0.3527	0.1508	0.1919	0.9132	0.9027	0.3012	0.3960
PRISM (emb_size=3072)	0.1927	0.2758	0.1348	0.1615	0.9325	0.9178	0.2727	0.3446
PRISM (emb_size=64)	0.0806	0.1261	0.0569	0.0715	0.7807	0.7222	0.1336	0.1869
DreamRec (emb_size=3072)	0.2416	0.3287	0.1767	0.2047	0.8620	0.8437	0.3054	0.3661
DreamRec (emb_size=64)	0.0814	0.1074	0.0651	0.0734	0.5744	0.5605	0.1268	0.1553
PreferDiff (emb_size=3072)	0.2531	0.3554	0.1818	0.2147	0.8925	0.8981	0.3228	0.3968
PreferDiff (emb_size=64)	0.1227	0.1841	0.0882	0.1078	0.8934	0.8788	0.1925	0.2595
Disco (emb_size=3072)	0.2678	0.3775	0.1983	0.2336	0.9823	0.9425	0.3466	0.4192
Disco (emb_size=64)	0.1171	0.1962	0.1107	0.1422	0.9916	0.9665	0.1895	0.2791
GossipCop								
GRU4Rec	0.2226	0.3194	0.1466	0.1778	0.8864	0.8706	0.2957	0.3678
SASRec	0.3078	0.4706	0.1607	0.2135	0.8743	0.8526	0.3612	0.4473
Bert4Rec	0.2372	0.3711	0.1338	0.1770	0.8764	0.8587	0.3078	0.3981
CL4SRec	0.2898	0.4100	0.1784	0.2174	0.8938	0.8932	0.3516	0.4275
PRISM (emb_size=3072)	0.2948	0.3447	0.2301	0.2463	0.8806	0.8733	0.3531	0.3852
PRISM (emb_size=64)	0.0023	0.0034	0.0015	0.0018	0.6570	0.6940	0.0046	0.0067
DreamRec (emb_size=3072)	0.4619	0.5501	0.3415	0.3704	0.8464	0.8336	0.4415	0.4742
DreamRec (emb_size=64)	0.0036	0.0049	0.0027	0.0031	0.5791	0.5903	0.0071	0.0096
PreferDiff (emb_size=3072)	0.4969	0.6022	0.3655	0.3999	0.8307	0.8228	0.4523	0.4887
PreferDiff (emb_size=64)	0.0084	0.0139	0.0053	0.0070	0.6542	0.7400	0.0164	0.0268
Disco (emb_size=3072)	0.5236	0.6143	0.3996	0.4292	0.9272	0.9039	0.4918	0.5207
Disco (emb_size=64)	0.0087	0.0162	0.0053	0.0077	0.7993	0.7993	0.0170	0.0311
MHMisinfo								
GRU4Rec	0.1151	0.1894	0.0760	0.0998	0.8380	0.8608	0.1803	0.2624
SASRec	0.1485	0.2592	0.0826	0.1179	0.8339	0.8915	0.2190	0.3276
Bert4Rec	0.1391	0.2299	0.0847	0.1138	0.8162	0.8786	0.2074	0.3017
CL4SRec	0.1734	0.2621	0.1101	0.1387	0.8577	0.9081	0.2469	0.3323
PRISM (emb_size=3072)	0.1700	0.2339	0.1181	0.1388	0.8398	0.8919	0.2418	0.3065
PRISM (emb_size=64)	0.0239	0.0295	0.0190	0.0208	0.7095	0.7317	0.0448	0.0546
DreamRec (emb_size=3072)	0.1819	0.2426	0.1313	0.1509	0.9002	0.8952	0.2633	0.3176
DreamRec (emb_size=64)	0.0282	0.0347	0.0233	0.0254	0.8281	0.8901	0.0528	0.0644
PreferDiff (emb_size=3072)	0.1974	0.2620	0.1389	0.1598	0.8693	0.8874	0.2713	0.3294
PreferDiff (emb_size=64)	0.0325	0.0380	0.0290	0.0308	0.8290	0.8989	0.0603	0.0701
Disco (emb_size=3072)	0.2215	0.2822	0.1580	0.1778	0.9305	0.9264	0.3000	0.3507
Disco (emb_size=64)	0.0123	0.0572	0.0074	0.0213	0.9968	0.9873	0.0240	0.1025

1070

1071

1072

more rapidly than the non-DM-based method SASRec (embedding size = 64). Specifically, Disco reaches its best performance at approximately the 40-th epoch, whereas SASRec requires around 400 epochs. This fast convergence rate of Disco partially offsets the additional computational cost introduced by high-dimensional embeddings.

1076

1077

In addition, we conducted further experiments to demonstrate that Disco can still achieve superior performance compared with non-DM-based methods when the embedding dimension is restricted to 64, as long as a minor modification is applied to the overall optimization objective. In particular, we augment Disco’s loss function with an additional Cross-Entropy term:

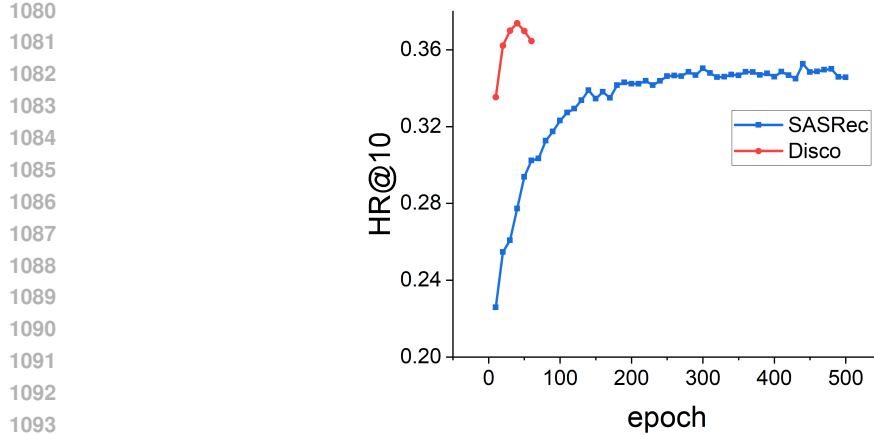


Figure 6: The performance convergence curve of SASRec and Disco on PolitiFact dataset.

Table 7: Performance comparison of Disco (optimized by $\mathcal{L}_{\text{Disco}^*}$) and non-DM recommendation methods on PolitiFact, GossipCop, and MHMisinfo when embedding dimension is set to 64.

Methods	HR@5	HR@10	NDCG@5	NDCG@10	CR@5	CR@10	HC@5	HC@10
PolitiFact								
GRU4Rec	0.2142	0.3390	0.1463	0.1863	0.9266	0.9122	0.2929	0.3889
SASRec	0.2158	0.3519	0.1386	0.1823	0.9059	0.9028	0.2923	0.3955
Bert4Rec	0.2191	0.3473	0.1472	0.1883	0.9127	0.9045	0.2960	0.3929
CL4SRec	0.2247	0.3527	0.1508	0.1919	0.9132	0.9027	0.3012	0.3960
Disco (emb_size=64, $\mathcal{L}_{\text{Disco}^*}$)	0.2335	0.3555	0.1642	0.2034	0.9316	0.9213	0.3111	0.4013
GossipCop								
GRU4Rec	0.2226	0.3194	0.1466	0.1778	0.8864	0.8706	0.2957	0.3678
SASRec	0.3078	0.4706	0.1607	0.2135	0.8743	0.8526	0.3612	0.4473
Bert4Rec	0.2372	0.3711	0.1338	0.1770	0.8764	0.8587	0.3078	0.3981
CL4SRec	0.2898	0.4100	0.1784	0.2174	0.8938	0.8932	0.3516	0.4275
Disco (emb_size=64, $\mathcal{L}_{\text{Disco}^*}$)	0.4250	0.5060	0.3320	0.3583	0.9151	0.9080	0.4407	0.4786
MHMisinfo								
GRU4Rec	0.1151	0.1894	0.0760	0.0998	0.8380	0.8608	0.1803	0.2624
SASRec	0.1485	0.2592	0.0826	0.1179	0.8339	0.8915	0.2190	0.3276
Bert4Rec	0.1391	0.2299	0.0847	0.1138	0.8162	0.8786	0.2074	0.3017
CL4SRec	0.1734	0.2621	0.1101	0.1387	0.8577	0.9081	0.2469	0.3323
Disco (emb_size=64, $\mathcal{L}_{\text{Disco}^*}$)	0.1856	0.2660	0.1214	0.1475	0.8669	0.9129	0.2599	0.3361

$$\mathcal{L}_{\text{Disco}^*} = \mathcal{L}_{\text{Disco}} - \log \left(\frac{\exp(f_\theta(\tilde{\mathbf{e}}_n^t, \mathbf{c}^{\text{pre}}, t) \cdot \mathbf{e}_n^\top)}{\sum_{i \in \mathcal{I}} \exp(f_\theta(\tilde{\mathbf{e}}_n^t, \mathbf{c}^{\text{pre}}, t) \cdot \mathbf{e}_i^\top)} \right). \quad (15)$$

The added term encourages the diffusion network f_θ to align its predictions more closely to the target items than with other items. Using this enhanced loss function $\mathcal{L}_{\text{Disco}^*}$, Disco can achieve better performance than non-DM based methods. The comparison results are reported in Table 7.

As shown in the Table 7, Disco can achieve better performance than non-DM recommendation methods with only a minor adjustment to its overall loss. This improvement arises because adding a discriminative loss (i.e., Cross Entropy loss) to the generative loss ($\mathcal{L}_{\text{Disco}}$) can partially mitigate the dimensionality limitations inherent to diffusion models.

1134 However, this practice will transform a purely generative model into a discriminative one. Our work
 1135 does not make such a compromise. Nevertheless, the results clearly suggest that our model retains
 1136 strong potential to surpass non-DM-based recommenders even when operating with substantially
 1137 reduced embedding dimensions. This highlights the potential of `Disco` to achieve an effective
 1138 trade-off between efficiency and performance.

1141 B.8 DISCUSSION ON DIFFUSION STEP T

1143 In this section, we conducted experiments to investigate whether `Disco` still strong performance
 1144 when the diffusion step T is much smaller. The experimental results are reported in Table 8.

1145 From Table 8, we can have the following observations:

- 1147 • As the diffusion step T increases, the performance of our proposed model, `Disco`, im-
 1148 proves.
- 1150 • `Disco` maintains superior performance compared with non-DM methods even at much
 1151 smaller diffusion step ($T=100$ for `PolitiFact` and `GossiCop`, and $T=500$ for `MHMisinfo`).

1155 Table 8: Performance comparison of `Disco` and non-DM recommendation methods under different
 1156 diffusion steps T .

1158 Methods	1159 HR@5	1160 HR@10	1161 NDCG@5	1162 NDCG@10	1163 CR@5	1164 CR@10	1165 HC@5	1166 HC@10
PolitiFact								
GRU4Rec	0.2142	0.3390	0.1463	0.1863	0.9266	0.9122	0.2929	0.3889
SASRec	0.2158	0.3519	0.1386	0.1823	0.9059	0.9028	0.2923	0.3955
Bert4Rec	0.2191	0.3473	0.1472	0.1883	0.9127	0.9045	0.2960	0.3929
CL4SRec	0.2247	0.3527	0.1508	0.1919	0.9132	0.9027	0.3012	0.3960
<code>Disco</code> (Diffusion step $T=100$)	0.2494	0.3724	0.1751	0.2146	0.9488	0.9352	0.3269	0.4146
<code>Disco</code> (Diffusion step $T=200$)	0.2602	0.3752	0.1842	0.2211	0.9427	0.9340	0.3353	0.4161
<code>Disco</code> (Diffusion step $T=500$)	0.2591	0.3828	0.1811	0.2208	0.9434	0.9272	0.3345	0.4193
<code>Disco</code> (Diffusion step $T=1000$)	0.2525	0.3784	0.1752	0.2156	0.9488	0.9369	0.3296	0.4186
<code>Disco</code> (Diffusion step $T=2000$)	0.2678	0.3775	0.1983	0.2336	0.9823	0.9425	0.3466	0.4192
GossipCop								
GRU4Rec	0.2226	0.3194	0.1466	0.1778	0.8864	0.8706	0.2957	0.3678
SASRec	0.3078	0.4706	0.1607	0.2135	0.8743	0.8526	0.3612	0.4473
Bert4Rec	0.2372	0.3711	0.1338	0.1770	0.8764	0.8587	0.3078	0.3981
CL4SRec	0.2898	0.4100	0.1784	0.2174	0.8938	0.8932	0.3516	0.4275
<code>Disco</code> (Diffusion step $T=100$)	0.4603	0.5479	0.3419	0.3705	0.9304	0.9252	0.4627	0.5016
<code>Disco</code> (Diffusion step $T=200$)	0.4759	0.5659	0.3537	0.3831	0.9242	0.9199	0.4689	0.5075
<code>Disco</code> (Diffusion step $T=500$)	0.4867	0.5798	0.3621	0.3925	0.9258	0.9169	0.4745	0.5120
<code>Disco</code> (Diffusion step $T=1000$)	0.4936	0.5956	0.3651	0.3984	0.9202	0.9039	0.4763	0.5139
<code>Disco</code> (Diffusion step $T=2000$)	0.5236	0.6143	0.3996	0.4292	0.9272	0.9039	0.4918	0.5207
MHMisinfo								
GRU4Rec	0.1151	0.1894	0.0760	0.0998	0.8380	0.8608	0.1803	0.2624
SASRec	0.1485	0.2592	0.0826	0.1179	0.8339	0.8915	0.2190	0.3276
Bert4Rec	0.1391	0.2299	0.0847	0.1138	0.8162	0.8786	0.2074	0.3017
CL4SRec	0.1734	0.2621	0.1101	0.1387	0.8577	0.9081	0.2469	0.3323
<code>Disco</code> (Diffusion step $T=100$)	0.1378	0.1998	0.0914	0.1111	0.8526	0.8783	0.2083	0.2746
<code>Disco</code> (Diffusion step $T=200$)	0.1393	0.2191	0.0921	0.1178	0.9161	0.9209	0.2136	0.2969
<code>Disco</code> (Diffusion step $T=500$)	0.1819	0.2610	0.1299	0.1553	0.9076	0.9144	0.2597	0.3323
<code>Disco</code> (Diffusion step $T=1000$)	0.2144	0.2638	0.1547	0.1708	0.9379	0.9311	0.2943	0.3358
<code>Disco</code> (Diffusion step $T=2000$)	0.2215	0.2822	0.1580	0.1778	0.9305	0.9264	0.3000	0.3507

1188 B.9 DISCUSSION ON VARIOUS RATIOS OF AVAILABLE CREDIBILITY LABELS
1189

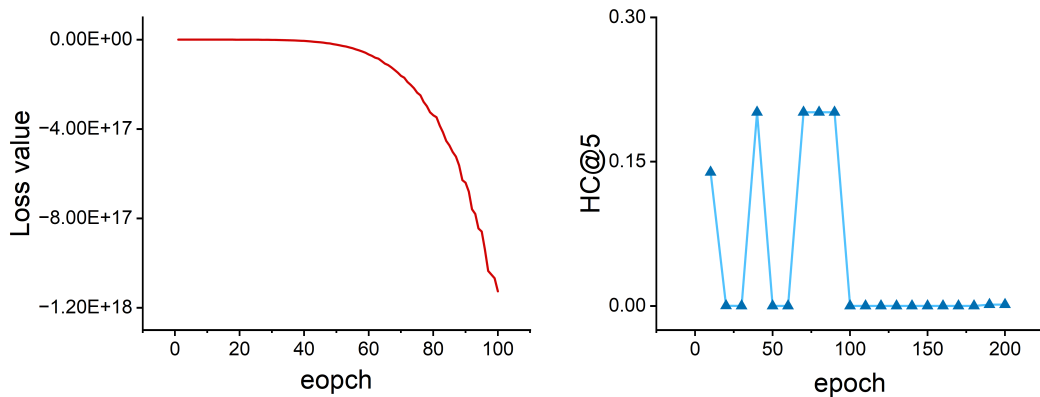
1190 we conduct additional experiments under different credibility label ratio of uncredible content (i.e.,
1191 5%, 10%, 20%, 30%, 50%). The experimental results are reported in Table 9. From the results
1192 reported in the Table, we can have the following findings:

1193

- 1194 • **Finding 1:** As the credibility label ratio increases, the recommendation credibility (CR)
1195 improves steadily. This is because a larger number of credibility labels enables the
1196 construction of a more comprehensive and accurate credible subspace, allowing uncredible
1197 content to be mitigated more effectively.
- 1198 • **Finding 2:** The recommendation accuracy fluctuates only slightly within a narrow range
1199 across different label ratios. This stability is attributed to our proposed disentangled
1200 diffusion model, which effectively mitigates uncredible content while preserving users'
1201 preference-related information, thereby maintaining high recommendation accuracy.

1202
1203
1204 Table 9: Performance comparison under different credibility label ratios.

1205 Label ratios	1206 HR@5	1206 HR@10	1206 NDCG@5	1206 NDCG@10	1206 CR@5	1206 CR@10	1206 HC@5	1206 HC@10
PolitiFact								
1207 5%	0.2617	0.3869	0.1819	0.2222	0.9422	0.9279	0.3365	0.4219
1208 10%	0.2541	0.3836	0.1768	0.2184	0.9476	0.9357	0.3308	0.4216
1209 20%	0.2678	0.3775	0.1983	0.2336	0.9823	0.9425	0.3466	0.4192
1210 30%	0.2704	0.3838	0.1980	0.2345	0.9829	0.9518	0.3489	0.4249
1211 50%	0.2678	0.3832	0.1923	0.2294	0.9842	0.9486	0.3468	0.4239
GossipCop								
1212 5%	0.5179	0.6021	0.4003	0.4279	0.9261	0.8726	0.4889	0.5060
1213 10%	0.5290	0.6115	0.4089	0.4359	0.9266	0.8764	0.4940	0.5105
1214 20%	0.5236	0.6143	0.3996	0.4292	0.9272	0.9039	0.4918	0.5207
1215 30%	0.5196	0.6141	0.3947	0.4255	0.9278	0.9101	0.4902	0.5227
1216 50%	0.5151	0.6069	0.3953	0.4253	0.9284	0.9176	0.4883	0.5226
MHMisinfo								
1219 5%	0.2127	0.2762	0.1500	0.1705	0.9149	0.9114	0.2904	0.3439
1220 10%	0.2112	0.2798	0.1506	0.1728	0.9217	0.9152	0.2897	0.3473
1221 20%	0.2215	0.2822	0.1580	0.1778	0.9305	0.9264	0.3001	0.3507
1222 30%	0.2207	0.2836	0.1551	0.1755	0.9303	0.9244	0.2994	0.3515
1223 50%	0.2134	0.2715	0.1533	0.1721	0.9331	0.9279	0.2929	0.3425

1238
1239
1240
1241 Figure 7: The loss and performance (HC@5) curves of variant w/o CE on PolitiFact dataset.

1242 B.10 DISCUSSION ON THE INSTABILITY OF ABLATION VARIANT w/o CE
1243

1244 In this section, we conduct an empirical study on the convergence of the ablation variant "w/o CE".
 1245 As show in Figure 7, we observe that the variant w/o CE (i.e., not replacing the MSE error with
 1246 cosine error) leads to extremely unstable training and performance. Specifically, the loss rapidly
 1247 collapses to an extremely small value (around -1.2×10^{18}), and the performance (HR@5) exhibits
 1248 severe fluctuations. These results verify the necessity of replacing the MSE error with the cosine
 1249 error to ensure stable optimization.

1250
1251 C WHY DMs POSE A DANGER OF GENERATING UNCREDIBLE CONTENT
1252 RECOMMENDATION?
1253

1254 In this section, we empirically and theoretically analyze why existing DM-based recommendation
 1255 methods risk generating uncredible recommendations.
1256

1257 C.1 EMPIRICAL FINDINGS
1258

1259 In DM-based recommendation methods, the condition and diffusion target are two critical factors.
 1260 In this section, we conduct experiments to examine how they influence the recommendation cred-
 1261 ibility of DM-based methods. Specifically, we divide the training dataset into four subsets based
 1262 on whether the context items or the diffusion target (i.e., target items) contain uncredible content.
 1263 We use \checkmark to denote that context items or target items contain uncredible content, and \times to denote
 1264 the opposite. After this dataset division, we train two representative DM-based recommendation
 1265 methods (DreamRec (Yang et al., 2023b) and PreferDiff (Liu et al., 2025a)) on each subset. From
 1266 the results reported in Table 10, we can find that these two factors indeed affect the recommenda-
 1267 tion credibility of DM-based methods. We refer to these two factors as uncredible condition and
 1268 uncredible diffusion target.

- 1269 • **Uncredible condition.** When controlling the diffusion target, if the context items contain uncredi-
 1270 ble content that leads to an uncredible condition, the credibility metric CR@10 (i.e., credible Rate)
 1271 decreases to some extent for both DreamRec and PreferDiff across the PolitiFact and GossipCop
 1272 datasets. This finding indicates that the uncredible condition is a factor contributing to the risk of
 1273 DMs generating uncredible recommendation results.
- 1274 • **Uncredible diffusion target.** When controlling the condition, if the diffusion target is an un-
 1275 credible item (i.e., an uncredible diffusion target), CR@10 drops to an extremely low level. This
 1276 further emphasizes that the uncredible diffusion target is another key contributing factor.

1277 Apart from these two findings, we also observe that training with the complete datasets yields worse
 1278 recommendation credibility compared to the subset where neither the condition nor the diffusion
 1279 target contains uncredible items. This further validates that the uncredible condition and the uncredi-
 1280 ble diffusion target are indeed the key contributing factors that place DM-based recommendation
 1281 methods at risk of generating uncredible recommendation results.

1282 Moreover, **although simply removing uncredible items from the datasets can improve recom-
 1283 mendation credibility, it significantly deteriorates recommendation accuracy.** This is because
 1284 uncredible items may also reflect users' genuine preferences, thereby discarding them restricts the
 1285 model's ability to accurately learn users' true interests. Therefore, it is crucial to design advanced
 1286 models that can mitigate the recommendation of uncredible content while simultaneously preserv-
 1287 ing high recommendation accuracy. This is the motivation and research significance of our proposed
 1288 model, Disco.

1290 C.2 THEORETICAL ANALYSIS
12911292 **Proof: Uncredible condition can enhance DM's generation of uncredible results**
1293

1294 The training of a conditional DM is to maximize $\mathbb{E}_{p_{data}(\mathbf{e}_n, \mathbf{c})} [\log p_{\theta}(\mathbf{e}_n | \mathbf{c})]$, where \mathbf{e}_n is the diffu-
 1295 sion target (i.e., the last item in a user's interaction sequence) and \mathbf{c} is the condition. This training
 objective pushes the generation toward the real data distribution.

1296

1297
1298
1299
Table 10: Performance comparison of DreamRec and PreferDiff under different settings of uncred-
ible content items in condition and diffusion target on PolitiFact and GossipCop datasets. Best results
are highlighted in bold.

Methods	Whether contain uncredible content items?		Politi				Gossip			
	condition	diffusion target	HR@10	NDCG@10	CR@10	HC@10	HR@10	NDCG@10	CR@10	HC@10
DreamRec	Training with complete dataset		0.3287	0.2047	0.8437	0.3661	0.5501	0.3704	0.8336	0.4742
	\times	\times	0.2674	0.1571	0.9935	0.3477	0.4658	0.3160	0.9771	0.4769
	\times	\checkmark	0.0577	0.0409	0.1888	0.0716	0.0372	0.0284	0.0522	0.0307
	\checkmark	\times	0.2671	0.1541	0.9875	0.3467	0.1927	0.1368	0.9340	0.2728
PreferDiff	\checkmark	\checkmark	0.0684	0.0413	0.0806	0.0507	0.0539	0.0404	0.0450	0.0317
	Training with complete dataset		0.3554	0.2147	0.8981	0.3968	0.6022	0.3999	0.8228	0.4887
	\times	\times	0.3035	0.1915	0.9591	0.3717	0.5036	0.3657	0.9315	0.4839
	\times	\checkmark	0.0557	0.0410	0.1073	0.0547	0.0407	0.0304	0.0833	0.0412
	\checkmark	\times	0.2625	0.1553	0.8561	0.3254	0.2074	0.1454	0.9076	0.2847
	\checkmark	\checkmark	0.0568	0.0385	0.0837	0.0482	0.0573	0.0421	0.0254	0.0208

1310

1311

1312
1313 When an uncredible content-related condition \mathbf{c}^{unc} is utilized to guide the generation process, the
model aims to maximize $\mathbb{E}_{p_{data}(\mathbf{e}_n, \mathbf{c}^{unc})} [\log p_{\theta}(\mathbf{e}_n | \mathbf{c}^{unc})]$. Then, we have:

$$\begin{aligned}
\mathbb{E}_{p_{data}(\mathbf{e}_n, \mathbf{c}^{unc})} [\log p_{\theta}(\mathbf{e}_n | \mathbf{c}^{unc})] &= \mathbb{E}_{p_{data}(\mathbf{c}^{unc})} \mathbb{E}_{p_{data}(\mathbf{e}_n | \mathbf{c}^{unc})} [\log p_{\theta}(\mathbf{e}_n | \mathbf{c}^{unc})] \\
&= \mathbb{E}_{p_{data}(\mathbf{c}^{unc})} \left[\int_{\mathbf{e}_n} p_{data}(\mathbf{e}_n | \mathbf{c}^{unc}) \log p_{\theta}(\mathbf{e}_n | \mathbf{c}^{unc}) d\mathbf{e}_n \right] \\
&= \mathbb{E}_{p_{data}(\mathbf{c}^{unc})} [-H(p_{data}(\mathbf{e}_n^* | \mathbf{c}^{unc}), p_{\theta}(\mathbf{e}_n^* | \mathbf{c}^{unc}))] \\
&= \mathbb{E}_{p_{data}(\mathbf{c}^{unc})} [-H(p_{data}(\mathbf{e}_n^* | \mathbf{c}^{unc}))] \\
&\quad - \mathbb{E}_{p_{data}(\mathbf{c}^{unc})} [D_{KL}(p_{data}(\mathbf{e}_n^* | \mathbf{c}^{unc}) \| p_{\theta}(\mathbf{e}_n^* | \mathbf{c}^{unc}))] \\
&= -H_{p_{data}}(\mathcal{E} | \mathcal{C}^{unc}) \\
&\quad - \mathbb{E}_{p_{data}(\mathbf{c}^{unc})} [D_{KL}(p_{data}(\mathbf{e}_n^* | \mathbf{c}^{unc}) \| p_{\theta}(\mathbf{e}_n^* | \mathbf{c}^{unc}))], \tag{16}
\end{aligned}$$

1324

1325
1326condition \mathbf{c}^{unc} . $H(\cdot, \cdot)$ is the entropy between two variables or distributions. According to the above
derivation, we have:

$$\begin{aligned}
H_{p_{data}}(\mathcal{E} | \mathcal{C}^{unc}) &= -\mathbb{E}_{p_{data}(\mathbf{e}_n, \mathbf{c}^{unc})} [\log p_{\theta}(\mathbf{e}_n | \mathbf{c}^{unc})] \\
&\quad - \mathbb{E}_{p_{data}(\mathbf{c}^{unc})} [D_{KL}(p_{data}(\mathbf{e}_n^* | \mathbf{c}^{unc}) \| p_{\theta}(\mathbf{e}_n^* | \mathbf{c}^{unc}))] \\
&\leq -\mathbb{E}_{p_{data}(\mathbf{e}_n, \mathbf{c}^{unc})} [\log p_{\theta}(\mathbf{e}_n | \mathbf{c}^{unc})]. \tag{17}
\end{aligned}$$

1331

1332
13331334 Ideally, when the model is optimally trained, the D_{KL} term will approach zero, indicating that the
conditional generation distribution approaches the real data distribution. Therefore, the mutual in-
formation between the whole conditional generation space \mathcal{E} and the whole uncredible condition
space \mathcal{C}^{unc} can be calculated as:

$$\begin{aligned}
I_{p_{\theta}}(\mathcal{E}, \mathcal{C}^{unc}) &= I_{p_{data}}(\mathcal{E}, \mathcal{C}^{unc}) \\
&= H_{p_{data}}(\mathcal{E}) - H_{p_{data}}(\mathcal{E} | \mathcal{C}^{unc}) \\
&\geq H_{p_{data}}(\mathcal{E}) + \mathbb{E}_{p_{data}(\mathbf{e}_n, \mathbf{c}^{unc})} [\log p_{\theta}(\mathbf{e}_n | \mathbf{c}^{unc})]. \tag{18}
\end{aligned}$$

1339

1340
1341
1342
1343
1344
1345
1346
The second equation is derived according to the property of mutual information: $I(X, Y) =$
 $H(X) - H(X|Y)$. As the training goes on, the second term becomes larger. At the same time,
 $H_{p_{data}}(\mathcal{E})$ is a constant based on the real data distribution p_{data} . Hence, the lower bound of
 $I_{p_{\theta}}(\mathcal{E}, \mathcal{C}^{unc})$ also becomes larger. Based on this, we can conclude that training the diffusion model
with uncredible conditions increases the mutual information between the generation space and the
uncredible condition space. This indicates that the generation space increasingly contains uncredible
features reflected in the uncredible conditions.1347
Proof: Uncredible diffusion target can enhance DM's generation of uncredible results1348
1349

The optimization loss of existing DM-based recommendation methods can be formulated as:

$$\mathcal{L} = \mathbb{E}_{t \sim U(0, T)} [\|\mathbf{e}_n^0 - f_{\theta}(\mathbf{e}_n^t, \mathbf{c}, t)\|_2^2]. \tag{19}$$

When an uncredible item embedding \mathbf{e}_j ($j \in \mathcal{I}_{unc}$) is used as the diffusion target (i.e., uncredible diffusion target) during training, the diffusion loss encourages the prediction direction of the diffusion network f_θ to move closer to \mathbf{e}_j . Specifically, the MSE distance between the diffusion target and the output of f_θ will be smaller, indicating higher similarity.

In the inference stage, the generation process of diffusion recommenders can be expressed as:

$$\mathbf{e}_n^{t-1} = w_1 f_\theta(\mathbf{e}_n^t, \mathbf{c}, t) + w_2 \mathbf{e}_n^t + w_3 \epsilon, \quad \epsilon \sim \mathcal{N}(\mathbf{0}, \mathbf{I}), \quad (20)$$

where $w_1 = \frac{\sqrt{\alpha_{t-1}}\beta_t}{1-\bar{\alpha}_t}$, $w_2 = \frac{\sqrt{\alpha_t}(1-\bar{\alpha}_{t-1})}{1-\bar{\alpha}_t}$, and $w_3 = \sqrt{\frac{1-\bar{\alpha}_{t-1}}{1-\bar{\alpha}_t}(1-\alpha_t)}$. This generation process is performed step by step, and the final embedding \mathbf{e}_n^0 is taken as the generation result, which then serves as the reference for item prediction and recommendations.

Let \mathbf{e}_n^{t-1} denote the generated embedding at step $t-1$ without using uncredible diffusion target \mathbf{e}_j during training. In such case, the parameters of the diffusion network are denoted as θ . Similarly, let $\hat{\mathbf{e}}_n^{t-1}$ denote the generated embedding at step $t-1$ with \mathbf{e}_j as the uncredible diffusion target during training. In this case, the diffusion parameters are denoted as $\hat{\theta}$. We then calculate the difference in similarity between the normalized \mathbf{e}_j and the normalized generated embeddings $\hat{\mathbf{e}}_n^{t-1}$ and \mathbf{e}_n^{t-1} at step $t-1$ as follows:

$$\begin{aligned} \Delta^{t-1} &= \text{sim}(\mathbf{e}_j, \hat{\mathbf{e}}_n^{t-1}) - \text{sim}(\mathbf{e}_j, \mathbf{e}_n^{t-1}) \\ &= [w_1 (f_{\hat{\theta}}(\hat{\mathbf{e}}_n^t, \mathbf{c}, t) - f_\theta(\mathbf{e}_n^t, \mathbf{c}, t)) + w_2 (\hat{\mathbf{e}}_n^t - \mathbf{e}_n^t) + w_3 (\epsilon^t - \epsilon)] \cdot \mathbf{e}_j^\top \\ &= w_1 (f_{\hat{\theta}}(\hat{\mathbf{e}}_n^t, \mathbf{c}, t) - f_\theta(\mathbf{e}_n^t, \mathbf{c}, t)) \cdot \mathbf{e}_j^\top + w_2 (\hat{\mathbf{e}}_n^t - \mathbf{e}_n^t) \cdot \mathbf{e}_j^\top. \end{aligned} \quad (21)$$

Here, we utilize the dot product to calculate the similarity. To avoid the interference from sampled noise, we use ϵ^t to denote the sample noise ϵ in step $t-1$, and use it for both generation processes to control this variable.

When $t = T$, we have:

$$\begin{aligned} \Delta^{T-1} &= \text{sim}(\mathbf{e}_j, \hat{\mathbf{e}}_n^{T-1}) - \text{sim}(\mathbf{e}_j, \mathbf{e}_n^{T-1}) \\ &= w_1 (f_{\hat{\theta}}(\hat{\mathbf{e}}_n^T, \mathbf{c}, T) - f_\theta(\mathbf{e}_n^T, \mathbf{c}, T)) \cdot \mathbf{e}_j^\top + w_2 (\hat{\mathbf{e}}_n^T - \mathbf{e}_n^T) \cdot \mathbf{e}_j^\top \\ &= w_1 (f_{\hat{\theta}}(\epsilon^T, \mathbf{c}, T) - f_\theta(\epsilon^T, \mathbf{c}, T)) \cdot \mathbf{e}_j^\top + w_2 (\hat{\mathbf{e}}_n^T - \mathbf{e}_n^T) \cdot \mathbf{e}_j^\top \\ &= w_1 (f_{\hat{\theta}}(\epsilon^T, \mathbf{c}, T) \cdot \mathbf{e}_j^\top - f_\theta(\epsilon^T, \mathbf{c}, T) \cdot \mathbf{e}_j^\top) \\ &= \underbrace{w_1}_{>0} \underbrace{(\text{sim}(\mathbf{e}_j, f_{\hat{\theta}}(\epsilon^T, \mathbf{c}, T)) - \text{sim}(\mathbf{e}_j, f_\theta(\epsilon^T, \mathbf{c}, T)))}_{>0} > 0. \end{aligned} \quad (22)$$

We control the process of two generations start from the same point $\hat{\mathbf{e}}_n^T = \mathbf{e}_n^T = \epsilon^T$ for fair comparison. As mentioned earlier, the prediction direction of $f_{\hat{\theta}}$ is closer to \mathbf{e}_j than that of f_θ . Hence, the MSE distance between the output of $f_{\hat{\theta}}$ and to \mathbf{e}_j is smaller than that between the output of f_θ and \mathbf{e}_j . When the embeddings are normalized, a smaller MSE distance corresponds to a higher dot product similarity. Consequently, $\text{sim}(\mathbf{e}_j, f_{\hat{\theta}}(\epsilon^T, \mathbf{c}, T)) - \text{sim}(\mathbf{e}_j, f_\theta(\epsilon^T, \mathbf{c}, T)) > 0$. At the same time, $w_1 > 0$, therefore $\Delta^{T-1} > 0$. This indicates that, when starting from the same initial point, the generation result at step $T-1$ produced by model $f_{\hat{\theta}}$, which has been trained with an uncredible diffusion target, will be more similar to this uncredible diffusion target.

When $t = T-1$, we have:

$$\begin{aligned} \Delta^{T-2} &= w_1 (f_{\hat{\theta}}(\hat{\mathbf{e}}_n^{T-1}, \mathbf{c}, T-1) - f_\theta(\mathbf{e}_n^{T-1}, \mathbf{c}, T-1)) \cdot \mathbf{e}_j^\top + w_2 (\hat{\mathbf{e}}_n^{T-1} - \mathbf{e}_n^{T-1}) \cdot \mathbf{e}_j^\top \\ &= w_1 C_{T-1}^+ + w_2 (\text{sim}(\mathbf{e}_j, \hat{\mathbf{e}}_n^{T-1}) - \text{sim}(\mathbf{e}_j, \mathbf{e}_n^{T-1})) \\ &= w_1 C_{T-1}^+ + w_2 \Delta^{T-1}. \end{aligned} \quad (23)$$

As mentioned before, when a uncredible item embedding \mathbf{e}_j is taken for training, the diffusion loss will encourage the prediction direction of $f_{\hat{\theta}}$ closer to \mathbf{e}_j . At the same time, $\hat{\mathbf{e}}_n^{T-1}$ is closer to \mathbf{e}_j , as compared to that of \mathbf{e}_n^{T-1} . This further enforces $f_{\hat{\theta}}(\hat{\mathbf{e}}_n^{T-1}, \mathbf{c}, T-1)$ more similar to \mathbf{e}_j , than that of $f_\theta(\mathbf{e}_n^{T-1}, \mathbf{c}, T-1)$. Hence, the first term is a positive constant, and we denote it by C_{T-1}^+ .

Similarly, when $t < T-1$, we have:

$$\begin{aligned} \Delta^{T-3} &= w_1 C_{T-2}^+ + w_2 \Delta^{T-2} \\ &= w_1 C_{T-2}^+ + w_2 (w_1 C_{T-1}^+ + w_2 \Delta^{T-1}) \\ &= w_1 C_{T-2}^+ + w_1 w_2 C_{T-1}^+ + w_2^2 \Delta^{T-1}. \end{aligned} \quad (24)$$

$$\begin{aligned}
1404 \quad \Delta^{T-4} &= w_1 C_{T-3}^+ + w_2 \Delta^{T-3} \\
1405 &= w_1 C_{T-3}^+ + w_2 (w_1 C_{T-2}^+ + w_1 w_2 C_{T-1}^+ + w_2^2 \Delta^{T-1}) \\
1406 &= w_1 C_{T-3}^+ + w_1 w_2 C_{T-2}^+ + w_1 w_2^2 C_{T-1}^+ + w_2^3 \Delta^{T-1}. \\
1407 &\dots
\end{aligned} \tag{25}$$

$$\begin{aligned}
1409 \quad \Delta^0 &= w_1 C_1^+ + w_1 w_2 C_2^+ + \dots + w_1 w_2^{T-2} C_{T-1}^+ + w_2^{T-1} \Delta^{T-1} \\
1410 &= \underbrace{\sum_m w_1 w_2^{m-1} C_m^+}_{>0} + \underbrace{w_2^{T-1} \Delta^{T-1}}_{>0} \\
1411 &= \text{sim}(\mathbf{e}_j, \hat{\mathbf{e}}_n^0) - \text{sim}(\mathbf{e}_j, \hat{\mathbf{e}}_n^0) \\
1412 &> 0.
\end{aligned} \tag{26}$$

According to above analysis, the final generated result $\hat{\mathbf{e}}_n^0$ using diffusion network $f_{\hat{\theta}}$ is more similar with uncredible item embedding \mathbf{e}_j , as compared to the final generated result \mathbf{e}_n^0 using diffusion network f_{θ} . This indicates that when uncredible items are used as the diffusion targets during training, the model tends to generate outputs that carry more uncredible features, i.e., embeddings that are more similar to uncredible items.

Algorithm 1 Training of Disco

```

1: Input: Training dataset  $\mathcal{S}_{train} = \{(\mathbf{e}_n, \mathbf{e}_{neg}, s^{pre}, s^{unc})\}_{s=1}^{|\mathcal{S}_{train}|}$ , available uncredible item
2: set  $\mathcal{I}_{unc}$ , trainable parameters  $\Theta$ , total diffusion steps  $T$ , learning rate  $\eta$ , variance schedules
3:  $\{\alpha_t\}_{t=0}^T$ .
4: Output: Optimized parameters  $\Theta$ .
5:  $\mathbf{F} = \text{Stack}(\{\mathbf{e}_i^{unc}\}_{i \in \mathcal{I}_{unc}})$  ▷ Construct uncredible feature matrix
6: repeat
7:    $(\mathbf{e}_n, \mathbf{e}_{neg}, s^{pre}, s^{unc}) \sim \mathcal{S}_{train}$  ▷ Sample training data
8:    $\mathbf{c}^{pre} = \text{Tramsformer}(s^{pre})$  ▷ Obtain preference-related condition
9:    $\mathbf{c}^{unc} = \text{Mean}(s^{unc})$  ▷ Obtain uncredible content-related condition
10:  Update  $\mathbf{F}$  by Algorithm 3 ▷ Progressive uncredible feature matrix enhancement
11:   $[\mathbf{U}_1; \mathbf{U}_2], \mathbf{\Lambda}, \mathbf{V} = \text{SVD}(\mathbf{F}^\top)$  ▷ Construct null space of uncredible feature matrix
12:   $\tilde{\mathbf{e}}_n = \mathbf{e}_n \mathbf{U}_2 \mathbf{U}_2^\top$  ▷ Credible subspace projection for diffusion target  $\mathbf{e}_n$ 
13:   $\tilde{\mathbf{e}}_n = (\tilde{\mathbf{e}}_n + \mathbf{e}_n)/2$  ▷ Residual connection
14:   $t \sim \text{Uniform}(1, T)$  ▷ Sample diffusion step
15:   $\tilde{\mathbf{e}}_n^t = \sqrt{\bar{\alpha}_t} \tilde{\mathbf{e}}_n^0 + \sqrt{1 - \bar{\alpha}_t} \epsilon$  ▷ Add noise to the embedding of diffusion target
16:   $\mathbf{e}_{neg}^t = \sqrt{\bar{\alpha}_t} \mathbf{e}_{neg}^0 + \sqrt{1 - \bar{\alpha}_t} \epsilon$  ▷ Add noise to the embedding of negative preference item
17:   $\Theta \leftarrow \Theta - \eta \nabla_{\Theta} \mathcal{L}_{\text{Disco}}(\tilde{\mathbf{e}}_n, \mathbf{e}_{neg}, \mathbf{c}^{pre}, \mathbf{c}^{unc}, t, \Theta)$  ▷ Update parameters
18: until convergence
19: return  $\Theta$ 

```

Algorithm 2 Inference of Disco

```

1: Input: Test dataset  $\mathcal{S}_{test} = \{s^{pre}\}_{s=1}^{|\mathcal{S}_{test}|}$ , trained diffusion network parameters  $\theta \in \Theta$ , total
2: reverse steps  $T$ , DDIM steps  $T'$ , variance schedules  $\{\alpha_t\}_{t=0}^T$ .
3: Output: A recommendation list for each user/sequence.
4:  $s^{pre} \sim \mathcal{S}_{test}$  ▷ Sample test sequence
5:  $\mathbf{c}^{pre} = \text{Transformer}(s^{pre})$  ▷ Obtain preference-related condition
6: for  $t' = T', \dots, 1$  do ▷ Calculate DDIM denoising step
7:    $t = \lfloor t' \times (T/T') \rfloor$  ▷ Start from Gaussian noise
8:    $\mathbf{e}_n^T \sim \mathcal{N}(\mathbf{0}, \mathbf{I})$ 
9:    $\mathbf{e}_n^{t-1} = \frac{\sqrt{\bar{\alpha}_{t-1}}(1-\alpha_t)}{1-\bar{\alpha}_t} f_{\theta}(\mathbf{e}_n^t, \mathbf{c}^{pre}, t) + \frac{\sqrt{\alpha_t}(1-\bar{\alpha}_{t-1})}{1-\bar{\alpha}_t} \mathbf{e}_n^t + \sqrt{\frac{1-\bar{\alpha}_{t-1}}{1-\bar{\alpha}_t}(1-\alpha_t)} \epsilon$  ▷ Step-by-step generation
10:   $\hat{y}_i = \mathbf{e}_n^0 \cdot \mathbf{e}_i^\top$  ▷ Calculate the matching score between a user/sequence and a candidate item  $\mathbf{e}_i$ 
11:   $\mathcal{R} = \{i | \text{TopK}(\hat{y}_i), i \in \mathcal{I}\}$  ▷ Select top K items with highest matching scores
12: return  $\mathcal{R}$ 

```

1458 **Algorithm 3** Progressive enhancement of uncredible feature matrix
1459 1: **Input:** Original uncredible feature matrix \mathbf{F} , available uncredible item set \mathcal{I}_{unc} , current iteration
1460 j , maximum selection ratio γ , maximum iteration m to reach γ .
1461 2: **Output:** Updated uncredible feature matrix \mathbf{F} .
1462 3: $UD(i) = \frac{1}{|\mathcal{I}_{unc}|} \sum_{i' \in \mathcal{I}_{unc}} \cos(\mathbf{e}_i^{unc}, \mathbf{e}_{i'}^{unc})$ \triangleright Calculate uncredible degree of items in $\mathcal{I} \setminus \mathcal{I}_{unc}$
1463 4: $ratio(j) = \min(\gamma, \frac{j}{m}\gamma)$ \triangleright Calculate the selection ratio at current iteration
1464 5: select $\lfloor |\mathcal{I} \setminus \mathcal{I}_{unc}| \cdot ratio(j) \rfloor$ items with highest uncredible degree \triangleright Select potential uncredible
1465 items
1466 6: Add potential uncredible items into \mathcal{I}_{unc} \triangleright Extension of uncredible item set
1467 7: $\mathbf{F} = \text{Stack}(\{\mathbf{e}_i^{unc}\}_{i \in \mathcal{I}_{unc}})$ \triangleright Enhancement of uncredible feature matrix
1468 8: **return** \mathbf{F}

1470
1471 **D DERIVATION OF EQUATION 5**
1472

1473
1474 In this section, we provide the derivation of Equation 5. For simplicity, we only need to derive
1475 the first term, since the derivation of the second term follows the same procedure. The detailed
1476 derivation is as follows:
1477

$$\begin{aligned}
& -\mathbb{E}_q \left[\log \frac{p_\theta(\mathbf{e}_n^{0:T} | \mathbf{c}^{pre})}{q(\mathbf{e}_n^{1:T} | \mathbf{e}_n^0)} \right] \stackrel{(1)}{=} -\mathbb{E}_q \left[\log \frac{p(\mathbf{e}_n^T | \mathbf{c}^{pre}) p_\theta(\mathbf{e}_n^0 | \mathbf{e}_n^1, \mathbf{c}^{pre}) \prod_{t>1}^T p_\theta(\mathbf{e}_n^{t-1} | \mathbf{e}_n^t, \mathbf{c}^{pre})}{q(\mathbf{e}_n^1 | \mathbf{e}_n^0) \prod_{t>1}^T q(\mathbf{e}_n^t | \mathbf{e}_n^{t-1}, \mathbf{e}_n^0)} \right] \\
& \stackrel{(2)}{=} -\mathbb{E}_q \left[\log \frac{p(\mathbf{e}_n^T | \mathbf{c}^{pre}) p_\theta(\mathbf{e}_n^0 | \mathbf{e}_n^1, \mathbf{c}^{pre}) \prod_{t>1}^T p_\theta(\mathbf{e}_n^{t-1} | \mathbf{e}_n^t, \mathbf{c}^{pre})}{q(\mathbf{e}_n^1 | \mathbf{e}_n^0) \prod_{t>1}^T \frac{q(\mathbf{e}_n^{t-1} | \mathbf{e}_n^t, \mathbf{e}_n^0) q(\mathbf{e}_n^t | \mathbf{e}_n^0)}{q(\mathbf{e}_n^{t-1} | \mathbf{e}_n^0)}} \right] \\
& \stackrel{(3)}{=} -\mathbb{E}_q \left[\log \frac{p(\mathbf{e}_n^T | \mathbf{c}^{pre}) p_\theta(\mathbf{e}_n^0 | \mathbf{e}_n^1, \mathbf{c}^{pre}) \prod_{t>1}^T p_\theta(\mathbf{e}_n^{t-1} | \mathbf{e}_n^t, \mathbf{c}^{pre})}{q(\mathbf{e}_n^1 | \mathbf{e}_n^0) \frac{q(\mathbf{e}_n^2 | \mathbf{e}_n^1)}{q(\mathbf{e}_n^1 | \mathbf{e}_n^0)} \cdots \frac{q(\mathbf{e}_n^T | \mathbf{e}_n^{T-1})}{q(\mathbf{e}_n^{T-1} | \mathbf{e}_n^0)} \prod_{t>1}^T q(\mathbf{e}_n^{t-1} | \mathbf{e}_n^t, \mathbf{e}_n^0)} \right] \\
& \stackrel{(4)}{=} -\mathbb{E}_q \left[\log p(\mathbf{e}_n^0 | \mathbf{e}_n^1, \mathbf{c}^{pre}) + \log \frac{p_\theta(\mathbf{e}_n^T)}{q(\mathbf{e}_n^T | \mathbf{e}_n^0)} + \log \frac{\prod_{t>1}^T p_\theta(\mathbf{e}_n^{t-1} | \mathbf{e}_n^t, \mathbf{c}^{pre})}{\prod_{t>1}^T q(\mathbf{e}_n^{t-1} | \mathbf{e}_n^t, \mathbf{e}_n^0)} \right] \\
& \stackrel{(5)}{=} -\mathbb{E}_q [\log p(\mathbf{e}_n^0 | \mathbf{e}_n^1, \mathbf{c}^{pre})] - \mathbb{E}_q \left[\log \frac{p_\theta(\mathbf{e}_n^T)}{q(\mathbf{e}_n^T | \mathbf{e}_n^0)} \right] \\
& \quad - \sum_{t>1}^T \mathbb{E}_q \left[\log \frac{p_\theta(\mathbf{e}_n^{t-1} | \mathbf{e}_n^t, \mathbf{c}^{pre})}{q(\mathbf{e}_n^{t-1} | \mathbf{e}_n^t, \mathbf{e}_n^0)} \right] \\
& \stackrel{(6)}{=} -\underbrace{\mathbb{E}_q [\log p(\mathbf{e}_n^0 | \mathbf{e}_n^1, \mathbf{c}^{pre})]}_{\text{reconstruction term}} + \underbrace{D_{\text{KL}}(q(\mathbf{e}_n^T | \mathbf{e}_n^0) \| p_\theta(\mathbf{e}_n^T))}_{\text{prior matching term}} \\
& \quad + \underbrace{\sum_{t>1}^T \mathbb{E}_q [D_{\text{KL}}(q(\mathbf{e}_n^{t-1} | \mathbf{e}_n^t, \mathbf{e}_n^0) \| p_\theta(\mathbf{e}_n^{t-1} | \mathbf{e}_n^t, \mathbf{c}^{pre}))]}_{\text{denoising matching term}}. \tag{27}
\end{aligned}$$

1505 Equation (2) is derived through Bayes rule: $q(\mathbf{e}_n^t | \mathbf{e}_n^{t-1}, \mathbf{e}_n^0) = \frac{q(\mathbf{e}_n^{t-1} | \mathbf{e}_n^t, \mathbf{e}_n^0) q(\mathbf{e}_n^t | \mathbf{e}_n^0)}{q(\mathbf{e}_n^{t-1} | \mathbf{e}_n^0)}$. Equation (4) is
1506 obtained since $p(\mathbf{e}_n^T | \mathbf{c}^{pre}) = p(\mathbf{e}_n^T)$ given $\mathbf{e}_n^T \sim \mathcal{N}(\mathbf{0}, \mathbf{I})$, which is independent with condition \mathbf{c}^{pre} .
1507

1508 DMs generally optimize the denoising matching term $D_{\text{KL}}(q(\mathbf{e}_n^{t-1} | \mathbf{e}_n^t, \mathbf{e}_n^0) \| p_\theta(\mathbf{e}_n^{t-1} | \mathbf{e}_n^t, \mathbf{c}^{pre}))$ in-
1509 stead of the whole variational bound. Then, this denoising matching term can be derived into the
1510 optimization loss $\mathcal{L} = \mathbb{E}_{\mathbf{e}_n^0, \mathbf{c}^{pre}, t} \left[\frac{1}{2\sigma_t^2} \|\boldsymbol{\mu}_q(\mathbf{e}_n^t, \mathbf{e}_n^0) - \boldsymbol{\mu}_\theta(\mathbf{e}_n^t, \mathbf{c}^{pre}, t)\|_2^2 \right]$, by adding the condition
1511 \mathbf{c}^{pre} into $\boldsymbol{\mu}_\theta(\mathbf{e}_n^t, t)$ in (Ho et al., 2020). Similar with (Pathak et al., 2023), $\boldsymbol{\mu}_q(\mathbf{e}_n^t, \mathbf{e}_n^0)$ is defined as

1512 (Pathak et al., 2023):
 1513

$$\mu_q(\mathbf{e}_n^t, \mathbf{e}_n^0) = \frac{\sqrt{\alpha_t}(1 - \bar{\alpha}_{t-1})\mathbf{e}_n^t + \sqrt{\bar{\alpha}_{t-1}}(1 - \alpha_t)\mathbf{e}_n^0}{1 - \bar{\alpha}_t}. \quad (28)$$

1516 In our model, $\mu_\theta(\mathbf{e}_n^t, \mathbf{c}^{pre}, t)$ is defined as:
 1517

$$\mu_\theta(\mathbf{e}_n^t, \mathbf{c}^{pre}, t) = \frac{\sqrt{\alpha_t}(1 - \bar{\alpha}_{t-1})\mathbf{e}_n^t + \sqrt{\bar{\alpha}_{t-1}}(1 - \alpha_t)f_\theta(\mathbf{e}_n^t, \mathbf{c}^{pre}, t)}{1 - \bar{\alpha}_t}, \quad (29)$$

1520 where $f_\theta(\mathbf{e}_n^t, \mathbf{c}^{pre}, t)$ is the predicted \mathbf{e}_n^0 using the diffusion network f_θ .
 1521

1522 Then, the optimization term can be rewritten as:
 1523

$$\begin{aligned} \mathcal{L} &= \mathbb{E}_{\mathbf{e}_n^0, \mathbf{c}^{pre}, t} \left[\frac{1}{2\sigma_t^2} \left\| \mu_q(\mathbf{e}_n^t, \mathbf{e}_n^0) - \mu_\theta(\mathbf{e}_n^t, t) \right\|_2^2 \right] \\ &= \mathbb{E}_{\mathbf{e}_n^0, \mathbf{c}^{pre}, t} \left[\frac{1}{2\sigma_t^2} \left\| \frac{\sqrt{\alpha_t}(1 - \bar{\alpha}_{t-1})\mathbf{e}_n^t + \sqrt{\bar{\alpha}_{t-1}}(1 - \alpha_t)\mathbf{e}_n^0}{1 - \bar{\alpha}_t} \right. \right. \\ &\quad \left. \left. - \frac{\sqrt{\alpha_t}(1 - \bar{\alpha}_{t-1})\mathbf{e}_n^t + \sqrt{\bar{\alpha}_{t-1}}(1 - \alpha_t)f_\theta(\mathbf{e}_n^t, \mathbf{c}^{pre}, t)}{1 - \bar{\alpha}_t} \right\|_2^2 \right] \quad (30) \\ &= \mathbb{E}_{\mathbf{e}_n^0, \mathbf{c}^{pre}, t} \left[\frac{1}{2\sigma_q^2(t)} \left\| \frac{\sqrt{\bar{\alpha}_{t-1}}(1 - \alpha_t)\mathbf{e}_n^0 - \sqrt{\bar{\alpha}_{t-1}}(1 - \alpha_t)f_\theta(\mathbf{e}_n^t, \mathbf{c}^{pre}, t)}{1 - \bar{\alpha}_t} \right\|_2^2 \right] \\ &= \mathbb{E}_{\mathbf{e}_n^0, \mathbf{c}^{pre}, t} \left[\frac{1}{2\sigma_q^2(t)} \left(\frac{\sqrt{\bar{\alpha}_{t-1}}(1 - \alpha_t)}{1 - \bar{\alpha}_t} \right)^2 \left\| \mathbf{e}_n^0 - f_\theta(\mathbf{e}_n^t, \mathbf{c}^{pre}, t) \right\|_2^2 \right]. \end{aligned}$$

1531 In practice, the coefficient $\frac{1}{2\sigma_q^2(t)} \left(\frac{\sqrt{\bar{\alpha}_{t-1}}(1 - \alpha_t)}{1 - \bar{\alpha}_t} \right)^2$ is generally omitted (Ho et al., 2020). Hence,
 1532 the optimization loss of our preference-related condition guided generation can be rewritten as
 1533 $\mathcal{L}_{pre} = \mathbb{E}_{\mathbf{e}_n^0, \mathbf{c}^{pre}, t} \left[\left\| \mathbf{e}_n^0 - f_\theta(\mathbf{e}_n^t, \mathbf{c}^{pre}, t) \right\|_2^2 \right]$. Similarly, the optimization loss of uncredible content-
 1534 related condition guided generation is: $\mathcal{L}_{unc} = \mathbb{E}_{\mathbf{e}_n^0, \mathbf{c}^{unc}, t} \left[\left\| \mathbf{e}_n^0 - f_\theta(\mathbf{e}_n^t, \mathbf{c}^{unc}, t) \right\|_2^2 \right]$. Our Disco
 1535 model aims to encourage the generation guided by preference-related condition and discourage the
 1536 generation guided by uncredible content-related condition. To achieve this goal, the optimization
 1537 objective is formulated as shown in Equation 5:
 1538

$$\mathcal{L} = \mathcal{L}_{pre} - \mathcal{L}_{unc} = \mathbb{E}_{\mathbf{e}_n^0, \mathbf{c}^{pre}, t} \left[\left\| \mathbf{e}_n^0 - f_\theta(\mathbf{e}_n^t, \mathbf{c}^{pre}, t) \right\|_2^2 \right] - \mathbb{E}_{\mathbf{e}_n^0, \mathbf{c}^{unc}, t} \left[\left\| \mathbf{e}_n^0 - f_\theta(\mathbf{e}_n^t, \mathbf{c}^{unc}, t) \right\|_2^2 \right]. \quad (31)$$

1550 E THEORETICAL JUSTIFICATION OF CREDIBLE SUBSPACE PROJECTION

1552 Our credible subspace projection is constructed using SVD. Applying SVD to the uncredible feature
 1553 matrix \mathbf{F}^\top yields the eigenvector matrix \mathbf{U} and the diagonal eigenvalue matrix Λ . \mathbf{U} and Λ can
 1554 be expressed as $\mathbf{U} = [\mathbf{U}_1; \mathbf{U}_2]$ and $\Lambda = \begin{bmatrix} \Lambda_1 & 0 \\ 0 & \Lambda_2 \end{bmatrix}$. Correspondingly, \mathbf{V} can be expressed as
 1555 $\mathbf{V} = [\mathbf{V}_1; \mathbf{V}_2]$. All zero or near-zero singular values are contained in Λ_2 , and the corresponding
 1556 eigenvectors are given by \mathbf{U}_2 and \mathbf{V}_2 .
 1557

1558 According to the principles of SVD, the following equation holds:
 1559

$$\mathbf{U}_2^\top \mathbf{F}^\top = \mathbf{U}_2^\top \mathbf{U}_1 \Lambda_1 \mathbf{V}_1^\top. \quad (32)$$

1562 Since the matrix \mathbf{U} obtained from the SVD is an orthogonal matrix, we have:
 1563

$$\mathbf{U}_2^\top \mathbf{F}^\top = \underbrace{\mathbf{U}_2^\top \mathbf{U}_1}_{=0} \Lambda_1 \mathbf{V}_1^\top = \mathbf{0}. \quad (33)$$

1566 Our credible diffusion target is derived through $\tilde{\mathbf{e}}_n = \mathbf{e}_n \mathbf{U}_2 \mathbf{U}_2^\top$. Hence, we have:
 1567

$$1568 \tilde{\mathbf{e}}_n \mathbf{F}^\top = \mathbf{e}_n \mathbf{U}_2 \underbrace{\mathbf{U}_2^\top \mathbf{F}^\top}_{=0} = 0. \quad (34)$$

1569
 1570

1571 This indicates that the derived credible diffusion target $\tilde{\mathbf{e}}_n$ is orthogonal to the uncredible feature
 1572 matrix \mathbf{F} . In summary, our proposed credible subspace projection effectively removes uncredible
 1573 content from the diffusion targets by ensuring that the projected targets lie orthogonally to the un-
 1574 credible content.
 1575

1576 F CASE STUDY

1577

1578 In this section, we conduct a case study using the GossipCop dataset to evaluate the effectiveness of
 1579 *Disco*. The GossipCop dataset contains users' interaction sequences with news articles, including
 1580 both true news (i.e., credible items) and fake news (i.e., uncredible items). Specifically, we present
 1581 the historical interaction sequences and recommendation lists for five users. The credible content
 1582 items are marked in green, while uncredible items are marked in red. In addition, to illustrate the
 1583 semantic relevance between content items, we utilize the same background color to highlight content
 1584 with similar or related topics. From Table 11, we have the following observations:
 1585

- 1586 • *Disco* demonstrates strong capability in delivering credible recommendations. Specifically, al-
 1587 though all these users have interacted with uncredible items in their historical interaction se-
 1588 quences, the recommendation lists generated by *Disco* contain no uncredible content.
 1589
- 1590 • *Disco* is capable of mitigating uncredible content while still preserving high recom-
 1591 mendation accuracy. This is achieved by removing uncredible features while retaining users' genuine
 1592 preference-related information. For example, taking User4 as an example, this user had histori-
 1593 cally interacted with some news (including fake news) about the death of celebrities (highlighted
 1594 in yellow). *Disco* can effectively capture this user's genuine preference and recommend some
 1595 content also in such topics. It is worth noting that User4 had interacted with fake news about the
 1596 death of "Tom Petty", and *Disco* recommends this user with a credible news article about the
 1597 same event. This plays an important role in countering misinformation, as it helps users correct
 1598 false impressions formed through prior exposure to uncredible content.
 1599

1600 G USAGE CLAIM OF LARGE LANGUAGE MODELS

1601

1602 We only utilize ChatGPT for polishing the academic writing, with the prompt "Proofread the gram-
 1603 mar and polish the writing of the given sentences".
 1604

1605
 1606
 1607
 1608
 1609
 1610
 1611
 1612
 1613
 1614
 1615
 1616
 1617
 1618
 1619

1620

1621 Table 11: Five cases showcasing the historical interaction sequences and the recommendation lists
 1622 of five users sampled from GossipCop dataset. **Credible** refers to credible content (i.e., true news)
 1623 and **Uncredible** refers to uncredible content (i.e., fake news). In a user sample, the texts marked
 1624 by the same-color background refer to similar topics. “**ground truth**” means the corresponding
 1625 recommended content items have been actually read by the user in the test set.

1626 1627 1628 1629 1630 1631 1632	User1	Historical sequence	Credible: Justin Timberlake, Chris Stapleton release 'Say Something' song , video.	Uncredible: Nicole Kidman, Keith Urban: Secrets to a Successful Relationship.	Uncredible: Kendall Jenner Shades Scott Disick Over Photo With Sofia Richie and His Kids.	Uncredible: Grammy winners 2018: the complete list.	
	Recommendations		Credible: 2018 Latin GRAMMY Awards Complete Winners List.	Credible: Weinstein Company Files for Bankruptcy and Revokes Nondisclosure Agreements.	Credible: Oscars: The Complete Winners List.	Credible: Pop superstar Lady Gaga has officially landed her first Las Vegas residency.	Credible (ground truth): TV News Roundup: Netflix Reveals Fuller House Season 4 Premiere Date
1633 1634 1635 1636 1637 1638 1639 1640 1641 1642	User2	Historical sequence	Credible: 13 Nights Of Halloween 2017 Schedule: Full List of Movies.	Uncredible: Taylor Swift will reportedly keep her new album off streaming services like Spotify and Apple Music for a week.	Uncredible: Former NBC interviewer lashes out at Trump in an NYT op-ed for reportedly casting doubt on the authenticity of the infamous tape.	Credible: 'Big Little Lies' Season 2 News, Premiere Date & Cast.	
	Recommendations		Credible (ground truth): Justin Timberlake Announces New Album Man of the Woods.	Credible: Seven-time and defending champion says she isn't quite ready to return after giving birth to daughter in September.	Credible: Pop superstar Lady Gaga has officially landed her first Las Vegas residency.	Credible: Jamie Lynn Spears' second child on the way will join big sister Maddie Briann.	Credible: "Good morning baby of mine, John Stamos' fiance Caitlin McHugh wrote as she debuted her baby bump...
1643 1644 1645 1646 1647 1648 1649 1650 1651 1652 1653	User3	Historical sequence	Credible: Hugh Grant and Anna Eberstein's baby on the way joins their daughter .	Uncredible: The cancellation of the third Sex and the City film came with headline-making fallout something Sarah Jessica Parker struggled with	Uncredible: Selena Gomez has completed her treatment for depression and anxiety and is reported feeling	Credible: Congratulations are in order for Rachel McAdams the 39-year-old actress is reportedly going to be a first-time mom! Though she has not personally confirmed the baby news	
	Recommendations		Credible: All Chicago West Baby Photos Timeline.	Credible: Demi Lovato Says She Contemplated Suicide at Age 7.	Credible: 'Black Panther' is the most tweeted about movie ever.	Credible (ground truth): His wife Faith Hill said the country star had been suffering from dehydration.	Credible: Tisha Campbell-Martin Files For Divorce From Husband of 21 Years
1654 1655 1656 1657 1658 1659 1660 1661 1662 1663	User4	Historical sequence	Uncredible: Caitlyn Jenner told Diane Sawyer that she had undergone the final surgery in her gender reassignment procedures on Friday night's 20/20 special.	Credible: Indiana police found the actress unresponsive after responding to a 911 call Saturday.	Credible: Roger Ailes, Former Fox News CEO, Dies At 77.	Uncredible: Tom Petty Dead: Celebrities React on Social Media Variety.	
	Recommendations		Credible: An emotional Celine Dion returned to the stage in Las Vegas on Tuesday night.	Credible (ground truth): Rocker Tom Petty died Monday after being rushed to a Los Angeles hospital.	Credible: Hugh Hefner's death certificate from the Los Angeles County Department of Public Health.	Credible: The final season of Netflix's "House of Cards" keeps the secret of how Frank Underwood died until the very end.	Credible: Pauley Perrette announces she's leaving "NCIS" after 15 seasons.
1664 1665 1666 1667 1668 1669 1670 1671 1672 1673	User5	Historical sequence	Credible: Benjamin Glaze had never kissed a girl before Katy Perry tricked him during the ABC reboot of American Idol.	Uncredible: During her chat with Ryan Murphy Friday (March 16) for the opening night of PaleyFest in Los Angeles.	Credible: A longtime aerialist for the famed Cirque Du Soleil plummeted to his death in front of a horrified crowd in Florida on Saturday night while trying out a new act...	Uncredible: Justin Bieber's struggling with his split from Selena Gomez as she's all smiles on her Australian vacation. Here's how the Biebs is coping with his...	
	Recommendations		Credible (ground truth): Justin Bieber Wants to Be With Selena Gomez But Is Hanging With Baskin Champion.	Credible: The singer covered Ariana Grande's 'Just a Little Bit of Your Heart' in the arena where her concert was attacked...	Credible: Trevorrow helmed the rebooted franchise's first installment.	Credible: Voting closes at 5pm PT today (June 29) for this year's News' TV Scoop Awards...	Credible: Blake Shelton Gets His Palms Read With Jimmy Fallon, Jokes About Having Too Much Sex.